

**PSYCHOPHYSICAL INFERENCE OF THE DIRECTION OF
NORMAL CONDUCTION IN THE SUBSTRATE FOR MEDIAL FOREBRAIN
BUNDLE SELF-STIMULATION**

Catherine Helen Bielajew

**A Thesis
in
The Department
of
Psychology**

**Presented in Partial Fulfillment of the Requirements
for the degree of Doctor of Philosophy at
Concordia University**

September, 1983

©Catherine Helen Bielajew, 1983

ABSTRACT

PSYCHOPHYSICAL INFERENCE OF THE DIRECTION OF
NORMAL CONDUCTION IN THE SUBSTRATE FOR MEDIAL FOREBRAIN
BUNDLE SELF-STIMULATION

Catherine Helen Bielajew, Ph.D.

Concordia University, 1983

Three experiments were conducted to assess the direction of normal propagation in the directly activated neurons responsible for the rewarding effects of medial forebrain bundle (MFB) stimulation in the rat. An anodal hyperpolarization block was produced by injecting current either rostral or caudal to MFB self-stimulation electrodes and the degree to which the hyperpolarizing current reduced the rewarding effect of stimulation was estimated using psychophysical measurement techniques. It was expected that a behaviorally effective block would occur if the anode were located between the cathode and the synapses of the directly stimulated cells responsible for the rewarding effect.

Monopolar stimulating electrodes were stereotaxically aimed at the lateral hypothalamus (LH) and ventral tegmental area (VTA). In the first experiment, the pulse-pair collision technique was employed to select those subjects in which the same reward related axons were fired

by both electrodes. The pulse-pair interval corresponding to a sudden increase in stimulation effectiveness was defined as the collision interval, the sum of the interelectrode conduction time and the refractory period. The latter was estimated in the second experiment using analogous procedures.

In the final study, pulses of different durations were applied using one of the depth electrodes as the cathode and the other as the anode. The effects of stimulating with this electrode configuration were compared to control conditions in which either electrode was used as the cathode and a skull screw was used as the anode.

With the VTA electrode serving as the anode and the LH electrode as the cathode, the effectiveness of stimulation was found to decline when the pulse duration approached or exceeded the interelectrode conduction time. No such effects were observed with a VTA cathode and an LH anode. This result was interpreted as evidence for rostrocaudal conduction in MFB fibers mediating brain-stimulation reward.

ACKNOWLEDGEMENTS

First, I thank my supervisor, Peter Shizgal, for his generous support and encouraging guidance throughout my graduate career. On a more local time scale, I also thank him for the blitz.

I have been indeed fortunate for the presence of Susan Schenk, a dear and cherished buddy and a respected colleague. On one level, her outrageous sense of humor and antics ensured never a dull moment in the lab. On another level, her willingness to listen, comment on, and critically evaluate my ideas are deeply appreciated.

To Dwayne Schindler, I am sincerely grateful for his tremendous support, particularly during the writing of this thesis. He generously placed himself at my disposal in order to be available at critical moments.

To other members of the laboratory - Ivan Kiss, Carol MacMillan, Stewart Francis, and David Morton - thank you for providing the lab with an atmosphere of friendship and comradery.

An endless list of gratitudes is owed George Fouriezos. First, he allocated a large chunk of his laboratory for my use so that I could comfortably conduct my experiments. Second, he never tired of discussing my data and coming to my rescue when equipment problems were overwhelming. Third, he devoted an inordinate amount of time, support, and encouragement towards the completion of

this thesis. For all of these things and much more, I am extremely thankful.

My debt is extended to the School of Psychology at the University of Ottawa for generously allowing me to make my presence felt the last three years, for supplying space in which to do so, and for permitting extensive use of their computer facilities.

My parents, Alina and Nicholas Bielajew, have provided emotional and monetary support that can never be repaid.

Finally, I wish to thank Diane Brazeau for secretarial services beyond the call of duty for this thesis and many past projects.

The financial backing of F.C.A.C. during the time these data were collected is acknowledged.

TABLE OF CONTENTS

	Page
ABSTRACT.....	i
ACKNOWLEDGEMENTS.....	iii
TABLE OF CONTENTS.....	v
LIST OF FIGURES.....	vii
LIST OF TABLES.....	viii
 INTRODUCTION.....	 1
Review of direction studies.....	10
Rationale for the direction experiment.....	19
Excitability cycles.....	21
Single cells.....	21
Population responses.....	22
Behavioral studies.....	25
Significance of behavioral data.....	29
Behavioral inference of anatomical linkage and conduction velocity.....	31
Anodal block technique.....	39
 EXPERIMENT 1.....	 58
Method.....	59
Subjects and surgery.....	59
Apparatus.....	60
Procedure.....	61
Screening and stabilization.....	61
Collision test.....	61
Pilot collision test.....	65
Data format.....	66
Histology.....	67
Results and Discussion.....	67
Histology.....	67
Pilot collision data.....	70
Collision data.....	72
Conduction velocity estimates.....	76
 EXPERIMENT 2.....	 79
Method.....	80
Subjects.....	80
Procedure.....	80
Data format.....	80

	Data analysis-asymptote test.....	81
	Data analysis-transformation procedure.....	82
	Results and Discussion.....	85
I.	Refractory period data.....	85
II.	Across-placement comparisons.....	88
	Statistical analysis-asymptote test.....	88
	Statistical analysis- transformed data.....	92
III.	Within-placement comparisons.....	96
	Statistical analysis-asymptote test.....	96
	Statistical analysis- transformed data.....	99
IV.	Conclusion.....	104
	EXPERIMENT 3.....	106
	Method.....	106
	Subjects.....	106
	Stimulation conditions.....	106
	Procedure.....	110
	Results and Discussion.....	110
	The shapes of the strength-duration functions.....	110
	The ratios of the strength-duration functions.....	118
	The timing of the block.....	119
	The position of the strength-duration curve on the ordinate.....	124
	Numerical description of the shape differences.....	130
	Anode-make excitation revisited.....	135
	Significance of these findings.....	137
	REFERENCES.....	139

LIST OF FIGURES

	Page
Figure 1. Illustration of possible interpretations in lesion experiments	15
Figure 2. Relationship between electrode alignment and collision profile	34
Figure 3. Hypothetical strength-duration curve ...	47
Figure 4. Explanation of anodal block technique ..	54
Figure 5. Relationship between single- and double-pulse train.....	63
Figure 6. Histology from Experiments 1, 2, and 3..	69
Figure 7. Within-subject comparison of E vs C-T curves for each collision test in Experiment 1	74
Figure 8. Within-subject comparison of E vs C-T curves for each placement in Experiment 2	87
Figure 9. Within-subject comparison of untransformed and transformed refractory period curves for each placement in Experiment 2	94
Figure 10. Refractory period curves regrouped to express placement and current differences	101
Figure 11. Within-subject comparison of current vs pulse duration for each stimulation condition tested at high currents in Experiment 3	113
Figure 12. Within-subject comparison of current vs pulse duration for each stimulation condition tested at low currents in Experiment 3	115
Figure 13. Hypothetical example of anode-make excitation.....	127

LIST OF TABLES

	Page
Table 1. Summary of results from Experiment 1...	71
Table 2. Minimum effectiveness value for each subject and placement in Experiment 2 ..	89
Table 3. Across-placement comparison of asymptote value for each subject in Experiment 2 ..	90
Table 4. F-test results from individual subject regression analysis of LH and VTA refractory period curves in Experiment 2	97
Table 5. T-test results from individual subject comparison of slopes of LH and VTA refractory period curves in Experiment 2	98
Table 6. F-test results from individual subject regression analysis of LH and VTA refractory period curves from high and low currents in Experiment 2	102
Table 7. Comparison of interelectrode conduction time and onset of anodal block effect for each subject in Experiment 3	120
Table 8. Individual subject chronaxie values derived from weighted regression analysis of each stimulation condition in Experiment 3	133
Table 9. Pearson r values associated with weighted regression analysis of each stimulation condition in Experiment 3 ..	134

INTRODUCTION

To cast light on the neural mechanisms underlying appetitively motivated behaviors, investigators have made extensive use of the self-stimulation paradigm. Contingent on a specific act such as lever pressing, a pattern of electrical pulses is applied to a designated brain site. Stimulation of the medial forebrain bundle (MFB) typically supports high rates of responding, and is often accompanied by the appearance of frenzied biting, licking, and chewing of the lever. If left undisturbed, subjects will often engage in lengthy episodes of almost continuous lever pressing.

The phenomenon of self-stimulation has been noted in a multitude of structures across a wide range of species from the fish (Boyd & Gardner, 1962) to homo sapiens (Bishop, Elder & Heath, 1963). While humans report a number of reactions to stimulation at sites homologous to those at which animals will self-stimulate, the underlying theme of their verbal descriptions is generally one of well-being and satisfaction.

In the self-stimulation paradigm, discrete regions of neural tissue are activated, raising the hope that one might directly access the circuitry mediating appetitively-motivated behavior. That there is a close relationship between brain-stimulation reward and

conventional rewards has been suggested by several findings. Stimulation at reward loci enhances approach to appetitive stimuli while attenuating withdrawal from noxious stimuli (Stellar, Brooks, & Mills, 1979). The avidity of self-stimulation is modified by some of the same factors that influence performance for natural rewards (Hoebel, 1974). For example, feeding and self-stimulation are both depressed by osmotic and gastric loads, while escape from aversive stimulation is enhanced by these manipulations (Hoebel & Thompson, 1975). Rolls, Burton, and Mora (1976) recorded the activity of basal forebrain neurons that responded to stimulation at brain-stimulation reward sites; they found that the presentation of food increased the activity of these cells but only when the subjects were food deprived. They concluded that the pathways mediating self-stimulation and feeding converge.

Uncovering the neural circuitry underlying brain-stimulation reward and the relationship between the functioning of this circuit and the effects of natural reinforcers is a major challenge for students of brain-behavior relationships. Before the operating principles of the circuit can be understood, its structure must first be determined. To accomplish this goal, one must first overcome a disquieting characteristic of stimulating at reward loci - the lack of specificity. Many of the sites that support self-stimulation also support eating (Hoebel &

Teitelbaum, 1962), drinking (Mendelson, 1967), exploration (Rompré & Miliaressis, 1980), circling (Miliaressis & Rompré, 1980), aversion (Bower & Miller, 1958), analgesia (Cooper & Taylor, 1967), or sexual behavior (Cagguila & Hoebel, 1966). While these findings are open to several interpretations, there is good reason to believe that at least in the medial forebrain bundle (MFB), all of these different behaviors are not mediated by the same cells (Bielajew & Shizgal, 1980; Durivage & Miliaressis, 1983).

The studies presented here attempt to trace the circuit(s) responsible for brain-stimulation reward by characterizing the neurophysiological properties of one of its segments. To do so, one must be able first to distinguish neurons responsible for the rewarding effect from other cells that are also activated by stimulation at reward loci.

A four stage strategy for doing this has been proposed by Gallistel, Shizgal, and Yeomans (1981). The first stage consists of establishing trade-off functions in order to place quantitative constraints on the neural population under examination. The second stage provides interpretations of the constraints in terms of anatomical and physiological properties. The third involves the direct recording of cellular activity in structures corresponding to those that yield the desired behavior. Finally the data collected in stage 3 are filtered using the characteristics

that were estimated in stage 2.

An example of how this approach has been applied in brain-stimulation reward studies can be seen in refractory period data obtained from stimulation of lateral hypothalamic (LH) sites. Yeomans (1975) derived the trade-off between the number of pulse pairs required to support a critical rate of lever pressing and the interpulse interval and related the shape of the function to the recovery from refractoriness in the underlying substrate. Kiss (1982) and Shizgal, Kiss, and Bielajew (1982) recorded population responses in the ventral tegmental area (VTA) that were triggered by stimulating electrodes in the LH and found that the time course of recovery from refractoriness was similar to that inferred by Yeomans (1975).

Given that many stages are likely to intervene between the reward-related neurons directly excited by the electrode and the behavioral consequences of stimulation, it may seem surprising that the characteristics of the first-stage elements can be inferred from self-stimulation performance. The logic underlying the notion that the properties of the directly stimulated tissue can be assessed from observation of the behavioral output has been discussed in detail by Gallistel et al. (1981). They argue that such inferences are valid if two requirements are met. First, data must be in the form of trade-off functions and, second, the relationship between the initial input and final output

must be monotonic. (The first restriction could be relaxed only in the extraordinary case where the behavioral output was linearly related to the excitation of the directly stimulated substrate. This point is taken up in detail on pages 25-29.)

Trade-off functions map pairs of stimulus parameters that produce the same outcome. An example is the function from which recovery from refractoriness is estimated. This function specifies the different pulse-pair frequencies and pulse-pair intervals that combine to produce a criterion level of self-stimulation performance. Firings lost due to refractoriness at short pulse-pair intervals are compensated by the addition of extra pulse pairs.

The behavioral trade-off function can be used to infer the properties of the underlying substrate only if the function observed behaviorally applies to every intervening stage. This condition is satisfied in a system built up of successive monotonic stages. In such a system, keeping the final output constant necessarily implies that the output of each intervening stage is likewise constant. If the output of the final or n^{th} stage is held constant, then the output of the $(n-1)^{\text{th}}$ stage must also be constant because the input of the n^{th} stage is the output of the $(n-1)^{\text{th}}$ stage and so on. In this fashion, constancy is maintained in each of the preceding states. The behaviorally derived trade-off

function can describe the recovery from refractoriness of the directly stimulated stage.

How can one know that the intervening stages are all monotonic? The introduction of nonmonotonocities at any intervening stage could not be corrected at later stages because information would be lost. In a nonmonotonic system, each output corresponds to more than one input; an observer stationed at or beyond the output of a nonmonotonic stage has no way of knowing which of the several possible inputs gives rise to a specific output. This argument implies that a monotonic relationship between the input to the first stage and the output of the last stage requires that all intervening steps also be monotonic.

In brain-stimulation reward studies, there is a monotonic relationship between the quantity of stimulation and the behavioral output over a wide range of input parameters that includes pulse duration, pulse frequency, and current intensity. These findings provide the justification for using constant output measures as an index of neurophysiological activity at the input stage. The reader is referred to the recent review by Gallistel et al. (1981) for a detailed discussion of the monotonicity argument.

The value of psychophysical inference is that it allows one to link the behavioral observations to neuronal functioning. While it would be relatively easier to

electrophysiologically record neural activity triggered by the stimulation, one could not know whether the neurons that give rise to the recorded signals are responsible for the rewarding effect of the stimulation or for one of the many other effects. Since the trade-off functions in psychophysical studies are behaviorally determined, they represent, in principle, only the properties of the cells mediating that behavior.

A growing list of self-stimulation structures has been examined in psychophysical studies. The excitability characteristics of reward-related neurons in the LH (Bielajew, Lapointe, Kiss, & Shizgal, 1982; Rompré & Miliaressis, 1980; Schenk & Shizgal, 1982; Yeomans, 1975; 1979), the periaqueductal gray (Bielajew, Jordan, Ferme-Enright, & Shizgal, 1981), the mediodorsalis (Bielajew & Fouriez, 1983), the nucleus accumbens (Bielajew, Walker, & Fouriez, 1983), and the medial prefrontal cortex (Schenk & Shizgal, 1982) have been estimated. The anatomical linkage between the substrates for self-stimulation of the LH and VTA (Bielajew & Shizgal, 1982; Shizgal, Bielajew, Corbett, Skelton, & Yeomans, 1980), the LH and periaqueductal gray (Bielajew et al., 1981), the LH and medial prefrontal cortex (Schenk & Shizgal, 1982), and the medial prefrontal and cingulate cortices (Silva, Vogel, & Corbett, 1982) have been examined and, when possible, conduction velocity estimates computed (Bielajew & Shizgal, 1982; Shizgal et

al., 1980). There have also been descriptions of strength duration relationships (Gallistel, 1978; Matthews, 1977; Milner & Laferrière, 1982; Schenk & Shizgal, 1983), temporal-integrating properties (Gallistel, 1978; Milner, 1978; Shizgal & Matthews, 1978), and current-distance relationships (Fouriezos & Wise, 1983).

The application of these procedures to other behaviors has yielded estimates of refractoriness for stimulation-induced escape (Skelton & Shizgal, 1980), circling (Miliaressis & Rompré, 1980), and exploration (Durivage & Miliaressis, 1983; Rompré & Miliaressis, 1980). Finally, the anatomical dissociation of the substrates for self-stimulation and stimulation-escape (Bielajew & Shizgal, 1980) and self-stimulation and exploration (Durivage & Miliaressis, 1983) has been inferred through the use of psychophysical methods. Some of these findings have been substantiated by direct electrophysiological recording (Shizgal et al., 1982). Furthermore, electron microscopic examination of tissue derived from self-stimulation regions is compatible with the above estimates (Nieuwenhuys, Geeraedts, & Veening, 1982; Szabo, Lénard, & Kosaras, 1974). That is, given the relationships between conduction velocity, refractory period, and axon diameter, a large proportion of axons are morphologically consistent with the behaviorally-derived neurophysiological characteristics.

The results of the above analyses have provided a

clearer view of the circuitry underlying brain-stimulation reward in the MFB. It appears that the substrate comprises, at least in part, small myelinated axons that directly link the LH and VTA. This interpretation questioned the direct involvement of catecholamine-containing neurons in the substrate for brain-stimulation reward. This notion was based largely on the considerable overlap of positive self-stimulation sites and the topography of midbrain dopamine trajectories (Corbett & Wise, 1980). Additional support was gained from pharmacological studies showing the changes in the vigor of self-stimulation following blockade of dopamine receptors (Fouriezos, Hansson, & Wise, 1978). However, the behaviorally derived MFB properties are incompatible with the electrophysiologically recorded estimates of the unmyelinated dopamine fibers which appear to be more difficult to excite, recover more slowly from refractoriness, and conduct at lower speeds (Dalsass, German, & Kiser, 1978; Feltz & Albe-Fessard, 1972; German, Dalsass, & Kiser, 1980; Guyenet & Aghajanian, 1978; Maeda & Mogenson, 1980; Takigawa & Mogenson, 1977; Yim & Mogenson, 1980). It may be that self-stimulation electrodes excite afferents to dopamine cells that, in turn, relay reward signals to forebrain or midbrain structures. Alternatively, dopamine fibers may modulate the activity of reward-related neurons without actually carrying reward signals.

The nature of the neurotransmitter substance

mediating the first stage neurons is unknown. (The first stage elements refer to the reward-related elements directly stimulated by the electrode.) Before attempting to identify the neurochemistry of the first stage reward neurons, it would be particularly useful to know the direction in which reward signals travel in order to reduce the number of candidate pathways. Anatomical linkage studies (Bielajew & Shizgal, 1982; Shizgal et al., 1980) suggest that the orientation of these fibers is longitudinal but whether the first stage cells project rostrally or caudally is unclear. It is the aim of this thesis to identify the direction of this projection. Before describing the strategy used here to address this question, a review of earlier studies will be presented.

Review of direction studies

The MFB is a heterogeneous collection of fiber systems with ascending and descending components (Nieuwenhuys, Geeraedts, & Veening, 1982; Veening, Swanson, Cowan, Nieuwenhuys, & Geeraedts, 1982). As such there are two views regarding the direction of normal propagation of reward signals, and each has its own antecedents. The view that fibers project rostrally is derived from the mapping and pharmacological studies mentioned earlier, while lesion experiments appear to favor a rostrocaudal direction. The conclusions from studies employing reversible lesions

induced by chemical injections have not been consistent; conflicting interpretations have also been drawn from studies in which electrical stimulation techniques have been used.

One difficulty that plagues the interpretation of much of this work concerns the use of scaling procedures that are rate dependent. That is, the majority of investigators have assessed the behavioral consequences of their manipulations by noting changes in the rate of lever pressing. This strategy does not allow one to distinguish between a reduction in the rewarding value of the stimulation and the animal's ability to perform the reward response. For example, Olds and Olds (1969) observed a striking impairment of response rates for MFB stimulation accompanying posterior lesions that was not apparent when tissue anterior to the stimulating electrode was destroyed. The failure to rule out performance factors (e.g., motoric disability) as a possible explanation for the decrement in responding weakens their interpretation that the first stage reward neurons follow a descending pathway.

A similar argument can be made with regard to the reversible lesion work. Nakajima (1972) and Stein (1969) examined response rates following application of procaine and lidocaine, local anaesthetics, to discrete MFB loci. Nakajima (1972) found that injections either in the LH or VTA, 1/2 mm above the electrode, attenuated performance for

stimulation at the uninjected site and concluded that both ascending and descending MFB pathways were critical to self-stimulation. Stein (1969) on the other hand reported that performance was more disrupted when lidocaine was delivered anterior to the stimulation site than when given more posteriorly, supporting the involvement of an ascending pathway. An alternative explanation for both of these studies is that the injections disrupted the ability of the animals to perform normally.

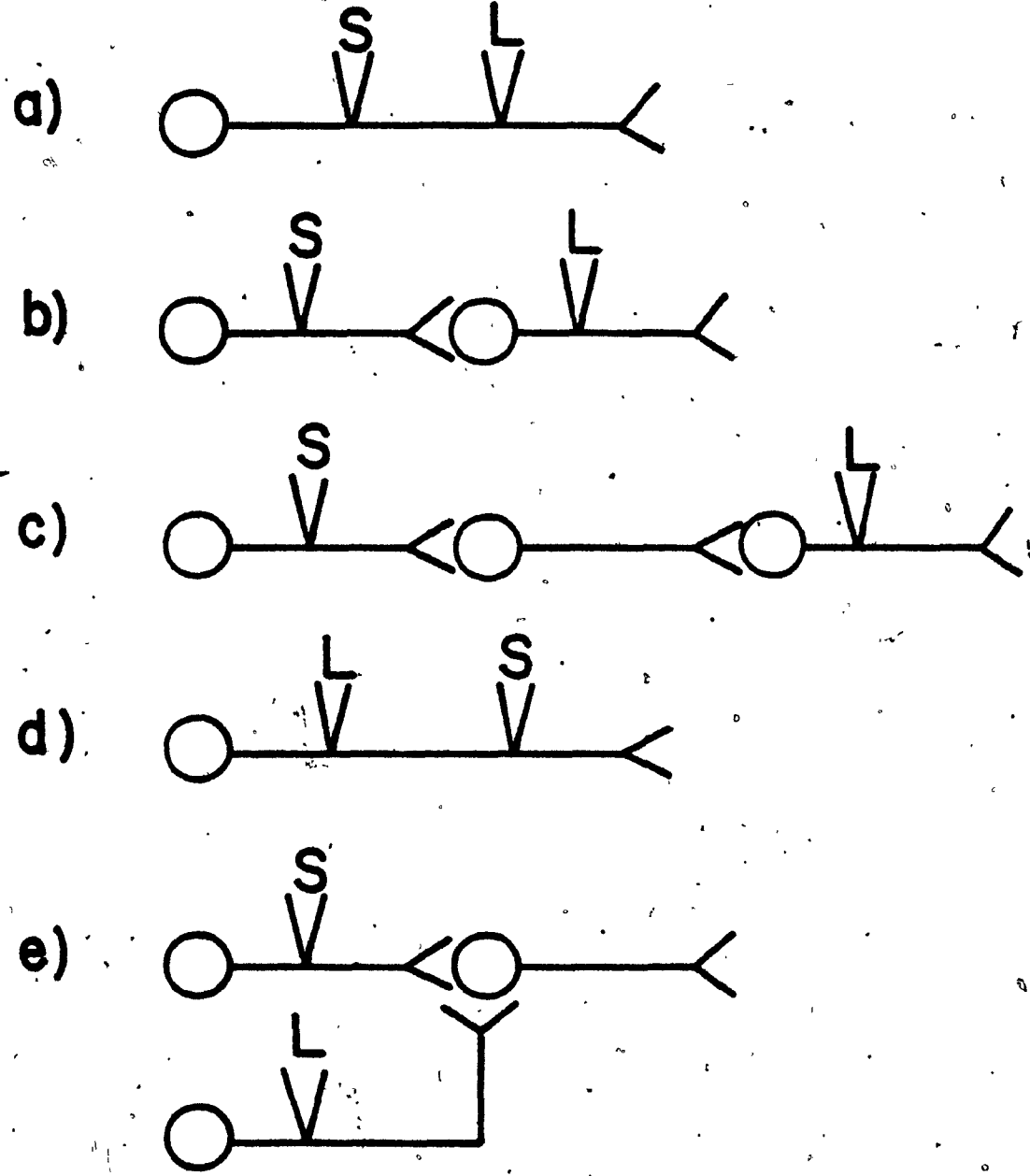
Measurement methods that can discriminate between changes in the animal's capacity to perform and changes in the rewarding value of stimulation (Edmonds & Gallistel, 1977) have been employed, albeit rarely. Stellar and Neeley (1981) placed electrolytic lesions anterior and posterior to MFB self-stimulation electrodes and found that the number of pulses required to sustain a constant running speed was greatly increased following posterior but not anterior lesions. Their findings are consistent with the notion that the effective lesions blocked conduction of reward signals generated in descending fiber projections. Nonetheless, the anatomical conclusions cannot be unambiguously drawn from the lesion data.

A weakness of the lesion approach is that it fails to indicate whether the stimulating and lesioning electrodes affect the same cells. Consider the diagrams in Figure 1. Whether the anatomical arrangements in Figure 1a, b, c, or d

represent the circuit under examination cannot be determined in a lesion experiment; behavior will be disrupted regardless of the position of the lesioning electrode. Moreover, electrodes located in the same pathway as in 1a and 1d but reversed so that the lesion in Figure 1a is between the stimulating electrode and the synapses while the lesion in Figure 1d is between the soma and the stimulating electrode would likely incur similar deficits. In Figure 1a, orthodromic impulses are prevented from propagating past the lesion; in Figure 1d, the axons under the stimulating electrode will have degenerated due to loss of contact with the cell bodies. On the basis of such results, one might incorrectly conclude that the fibers critical to behavior project both caudally and rostrally. Finally, it is possible that the integrity of self-stimulation pathways depends on the input of several converging pathways, as in Figure 1e. While the pathway in which the stimulating electrode is located has been spared by the lesion, the impulses generated in that bundle are ineffective unless accompanied by signals from the pathway destroyed by the lesion. The results from Huston and Borbély's (1973, 1974) heroic preparation are often cited as a supporting argument for the notion that the fibers related to reward project towards the brainstem. Rats with bilateral ablation of the major forebrain structures including the cortex, hippocampus, striatum and septum successfully learned to make various

Figure 1: Hypothetical examples to illustrate difficulty of making unambiguous conclusion from lesion results. The same conclusion is consistent with a variety of stimulating and lesioning electrode positions.

S = STIMULATING ELECTRODE
L = LESIONING ELECTRODE



responses for hypothalamic stimulation. Despite their sorry state, the animals usually displayed acquisition within the first half-hour of training. This finding questions the role of the ascending dopaminergic pathways in the substrate for MFB self-stimulation since all of the dopamine terminal fields in the forebrain were removed or damaged. Of course it is possible that other ascending pathways relevant to the behavior were spared.

Recently, Stellar, Illes, and Mills (1982) examined preparations similar to Huston and Borbély's (1973, 1974) except that the ablations were restricted to one hemisphere. Using psychophysical measures to assess the degree of impairment of self-stimulation from LH electrodes in the lesioned side, they surprisingly observed normal trade-off functions between the current and the number of pulses, and between the current and the train duration. Thus, despite the extensive unilateral damage in these animals, the characteristics of the LH reward substrate remained unchanged. Because the origins of some of the major descending trajectories were missed by their ablations, one hypothesis entertained by Stellar et al. (1982) is that the path along which reward signals propagate is descending. Alternatively, the substrate for these rewarding effects comprise ascending or descending fibers that cross the midline.

Finally, electrical stimulation techniques have

been used by German and Holloway (1972) and Szabo, Nad, and Szabo (1972) to infer direction although the design and conclusion are different in each study. German and Holloway (1972) based their conclusion of rostrocaudal conduction on the pattern of responding for double pulses delivered concurrently to the preoptic area and the contralateral lateral hypothalamus. By varying the spacing between paired pulses, a slight facilitation of rate was found when the first pulse of each pair was delivered to the anterior electrode 1.5 msec before the application of the second pulse to the posterior electrode. A similar enhancement was not noted when the order of presentation of the pulses was reversed. They argued that their result reflects the convergence of simultaneously arriving impulses at a location posterior to the stimulating electrodes. This study illustrates the problem of using response scaling as an index of neuronal activity. Using constant output procedures, Shizgal et al. (1980) delivered pulse pairs of different intervals to bilateral LH sites. According to German and Holloway (1972) the function relating the behavioral effectiveness of stimulation to pulse-pair interval should have declined as the interval was increased. Instead, Shizgal et al. (1980) found no change in effectiveness across a wide range of pulse-pair intervals. The measurement methods and statistical procedures used by German and Holloway (1974) have been discussed by Yeomans

and Koopmans (1974).

In principle, the logic underlying the Szabo et al. (1972) experiment shares many similarities with the direction test reported in this thesis. They assessed the effectiveness of bipolar stimulation delivered to electrodes aligned longitudinally in the LH, and found higher current thresholds when the anterior electrode served as the anode, suggesting that the more important direction for reward impulses is ascending. The omission of critical controls, however, mitigates this view. One alternative explanation for their data is that the density of reward relevant fibers was higher at the anterior electrode than at the posterior electrode. Consequently less current was required to support criterial performance at the anterior site.

A second possibility is that their electrodes lesioned the critical pathway. The coordinates were based on the method of De Groot which fixes the animal's head in a stereotaxic position so that the interaural line is 5 mm below the upper incisor bar. The electrodes however were cut so that the tips, separated by 0.2 mm, remained in the same horizontal plane. Since the MFB is roughly parallel to the surface of the brain, the excursion of the more anterior electrode might have damaged a significant portion of the fibers running under the tip of the posterior electrode.

It is plain from this discussion that a clear demonstration of the direction of normal conduction of MFB

reward fibers is lacking. The inherent difficulties of interpretation with many of the procedures and the use of behavioral output measures renders most conclusions ambiguous.

Rationale for the direction experiment

Experiment 3 of this dissertation employs constant output procedures to determine the direction in which the directly stimulated neurons mediating MFB stimulation project. The anodal block procedure is applied using two self-stimulation electrodes along the MFB, each of which serves either as the anode or the cathode. The inference of direction is based on the degree to which the hyperpolarization induced by the anode reduces the rewarding effect of stimulation at the cathode. Provided that the electrodes affect some of the same reward-related fibers, hyperpolarizing current should prevent impulses from reaching the synapses of the reward-related neurons when 1) the anode is located between the cathode and the critical synapses, and 2) the pulse duration equals or exceeds the interelectrode conduction time.

The first and second experiments serve as prerequisites for the direction test in that they identify electrode pairs and currents that stimulate some of the same reward-related neurons at two levels of the MFB and estimate the time required for impulses to traverse the segments of

these neurons between the two electrodes. The collision experiment, conducted first, selects animals in which reward-related axons directly link the LH and VTA stimulation fields. Such an arrangement is inferred when lengthening the C-T interval yields a sudden increase in the effectiveness of double-pulse stimulation. The interval between pulses at which this event occurs is termed the collision interval, the sum of the interelectrode conduction time and the refractory period. The latter is estimated in the second study, and when subtracted from the collision interval, yields an estimate of the conduction time between electrodes.

The next sections summarize the principal physiological phenomena, measurement methods, and findings relevant to each of the three experiments. Although recovery from refractoriness was estimated in the second experiment, the scaling principles underlying all three experiments were developed in refractory period studies. To facilitate the exposition of the measurement procedures, the section on excitability cycles will precede a discussion of collision experiments. This is the reverse order in which the studies were conducted and reported in this thesis.

Excitability cycles

Single cells. The following describes the post-stimulation excitability cycle of a single axon. First, a few terms need to be defined. The development of paired-pulse techniques to assess the excitability of neurons has given rise to the convention of naming the first pulse the C pulse, because it sets up the conditions that will be tested by the second, or T pulse. Plotting the inverse of the T-pulse threshold as a function of C-T interval yields an excitability curve.

The application of a subthreshold C pulse produces a local nonpropagating disturbance in membrane potential that decays as a function of the time constant of the membrane. However, a suprathreshold depolarization due to summation of a pair of subthreshold stimuli may occur if the delay between stimuli is sufficiently brief (Lucas, 1910). C pulses of suprathreshold amplitude initiate a series of successive events. The first corresponds approximately to the duration of the action potential and is termed the absolute refractory period; during this phase the membrane is unresponsiveness to further (T pulse) stimulation. The next stage is the relative refractory period; the membrane, now somewhat excitable, will fire in response to T pulses if their amplitude is greater than that of the C pulse. Following the relative refractory period, a supernormal period is observed in certain classes of fibers (Eyzaguirre

& Fidone, 1975). The membrane appears hyperexcitable and will fire in response to T pulses with amplitudes lower than the C-pulse threshold. The length of the supernormal period may be related to the type of the fiber. The final event is the subnormal period, an interval when the T-pulse threshold is again elevated. At least in the peripheral nervous system, wide differences in the degree of hypoexcitability of the membrane have been reported during the subnormal phase have been reported (Gasser & Grundfest, 1936; Raymond & Lettvin, 1972).

Population responses. If one assumes that an electrode activates a homogeneous population of fibers the above description of excitability following stimulation of single axons can be generalized to the more meaningful case, with respect to behavioral studies, of stimulation of a population of fibers.

Imagine that an electrode is located in the middle of a bundle of equally excitable fibers, uniformly distributed in space. The electrode tip can be thought to directly influence three regions within the fiber bundle. Nearest the tip where current density is greatest, all neurons will fire in response to both C and T pulses as long as the interval between pulses exceeds the absolute refractory period of the fibers. The second region is located further from the electrode tip and corresponds to an area of lower current density. At the inner border of this

region, fibers are excited during the early portion of the relative refractory period; at the outer border of this region, where current density is lower, fibers are excited only at the end of the relative refractory period. Finally, local potential summation may occur in the outlying region where the current density is inadequate to produce C-pulse firings. In this region, the summation of two depolarizations in close temporal contiguity may surpass the required threshold for excitation and produce firings.

Now suppose that stimulation of this bundle gives rise to a muscle contraction. The results of double-pulse stimulation can be inferred from the activity of the muscle. In fact, before the development of the oscilloscope which permitted detailed and accurate recording of the compound action potential (Erlanger & Gasser, 1939), neurophysiologists at the turn of the century routinely inferred the recovery characteristics of the nerve from observation of the muscle (Adrian & Lucas, 1912; Boycott, 1899; Bramwell & Lucas, 1911; Gotch & Burch, 1899; Lucas, 1910).

For purposes of this discussion, assume that the C pulse intensity is adjusted so that it is just insufficient to produce a detectable contraction when a single C pulse is delivered, and yields a clearly detectable contraction when two C pulses, widely separated in time, are delivered. At extremely short C-T intervals, a contraction might be

observed due to the summation of subthreshold local potentials. When the C-T interval is increased but within the absolute refractory period, the muscle will fail to be activated because the T pulse will fail to stimulate any neurons. Intervals that just exceed the absolute refractory period of neurons in the region nearest the tip should cause an observable contraction. The amplitude of the contraction will increase steadily as the C-T interval is pushed farther into the relative refractory period range and the border of the stimulation field produced by the T pulse sweeps through the second region described above. A full-sized contraction will only be observed when the C-T interval surpasses the relative refractory period.

The interpretation of double-pulse stimulation is more complicated when the density of fibers varies from region to region; the contribution of the various phases of excitability will now depend on the distribution of fibers within each region. A large proportion of neurons near the tip will elicit a sizeable muscle contraction at C-T intervals just greater than the absolute refractory period. In contrast, if the largest proportion is further from the tip, no response will be elicited until the absolute refractory periods and at least part of the relative refractory periods are exceeded. The magnitude of local potential summation will depend on the relative densities of fibers in the subliminal fringe and the suprathreshold

regions.

The detection of the remaining phases of excitability requires a modification of the double-pulse procedure and is beyond the scope of this thesis. The reader is referred to Yeomans (1979) for a detailed explanation.

The above description of how motoneuron excitability is indirectly inferred from muscle behavior is analogous to the manner in which the excitability of first stage reward neurons is estimated from self-stimulation. A critical difference concerns the dependent measure. In the above example, the output of the dependent measure is the magnitude of the contraction which is readily measured by standard transducers. In contrast, the relevant output is less obvious in brain-stimulation reward studies. The question of how to scale the performance of the self-stimulating rat is discussed in the following section.

Behavioral studies. The use of pulse-pair techniques for assessing the neurophysiological character of central reward neurons was pioneered by Deutsch (1964). He had the idea that one could indirectly derive the excitability characteristics of cells activated by rewarding brain stimulation from changes in an animal's response rate brought about by varying the C-T interval. Three experiments were conducted, using three different response requirements. One of the main findings was that the range of C-T intervals at which performance was enhanced appeared to depend on the

paradigm employed.

His study was followed by estimates of recovery for other stimulation produced behaviors (Hawkins & Chang, 1975; Hu, 1973; Rolls, 1973; Rolls & Kelley, 1972; Schmitt, Sander, & Karli, 1976). In each instance, the range of C-T intervals over which performance increased was defined as the upper and lower boundaries of the refractory period.

Yeomans (1975) challenged the methods employed in the early studies. He argued that the use of the dependent measure as an index of the rewarding impact of stimulation relies on the unwarranted assumption that the level of responding is linearly related to the total excitation in the neural substrate. In fact, the relationship between response rate and the frequency of stimulation is non-linear over a large range of frequencies. At extreme ends of the range, floor and ceiling effects are exhibited. As a result, an estimate of recovery from refractoriness based on a single frequency will be a function of this parameter. As a demonstration of this dependency, Yeomans collected refractory period data at nine different frequencies and obtained nine different estimates of recovery. No effect of C-T interval was observed using frequencies in the floor and ceiling range, which correspond to minimum and maximum response levels. This startling finding weakens the conclusions that can be drawn from refractory period studies based on response rates.

A solution for obtaining more consistent measures of recovery was proposed by Yeomans. He suggested a different method of scaling refractory period data. Holding the C-T interval constant, the frequency was varied and the response rate recorded. A family of functions relating frequency to response rate was generated, each representing a different C-T interval. He found that as the C-T interval increased, the rate versus frequency curves shifted to the left. To describe this pattern, he determined the frequency that corresponded to a criterion level of responding for each curve. Each of these frequencies was then compared to the frequency associated with trains composed solely of C pulses. In this manner, an effectiveness function was computed. The computational formulae are given below.

Yeomans's scaling procedure requires a few simple assumptions - that response rate is monotonically related to the total level of excitation and that the behavioral weight of each pulse is invariant over the tested range of frequencies. Empirical support for these assumptions has been reported (Gallistel, 1978; Hawkins, Roll, Puerto, & Yeomans, 1983).

Using this method to reassess the data collected at different frequencies, Yeomans found for the same placement, little across-subject variation in data obtained from a given site; good agreement in estimates collected in different laboratories has also been noted (Bielajew et al.,

1981; Rompré & Miliaressis, 1980).

Yeomans's procedure for estimating excitability using constant behavioral output has enjoyed many applications. It has been used to document recovery from refractoriness at a variety of brain-stimulation reward sites (Bielajew & Fouriez, 1983; Bielajew et al., 1982; Bielajew et al., 1983; Bielajew & Shizgal, 1982; Silva et al., 1982; Durivage & Miliaressis, 1983; MacMillan & Shizgal, 1983; Schenk & Shizgal, 1982) to characterize the substrates for other stimulation-produced behaviors (Miliaressis & Rompré, 1980; Rompré & Miliaressis, 1980; Skelton & Shizgal, 1980), and finally, to dissociate the rewarding effects of stimulation from stimulation escape (Skelton & Shizgal, 1980) and exploration (Rompré & Miliaressis, 1980) at the same locus.

The theoretical basis for Yeomans's improved scaling method is derived from a consideration of the counter model (Gallistel, 1973; Yeomans, 1974). Impulses are generated in a "cable", which constitutes the directly stimulated fibers underlying the rewarding effect. Elsewhere in this thesis, I have referred to the cable as the "first-stage reward neurons". The postsynaptic consequences are computed by the integrator, a mechanism that sums signals temporally and spatially; the output of the integrator is the reward signal. The integrator can record the same effect from different patterns of stimulation. For

example, given a constant train duration twenty neurons that contribute five impulses each have the same impact as ten neurons that each contribute ten impulses. Provided that performance conditions do not change, a constant behavioral output will ensure the same integrator signal, even though the values of parameter that generate the signal vary. In refractory period studies, the same integrator output is maintained at all C-T intervals by adjusting the number of pulse pairs. As the C-T interval is decreased, additional pulse pairs are added to replace firings lost due to refractoriness.

To give a numerical example, the refractory period is deemed complete when 25 pulse pairs are behaviorally equivalent to 50 single pulses. This indicates that each T pulse is as effective as each C pulse. During the absolute refractory period, 50 pulse pairs should be behaviorally equivalent to 50 single pulses. This indicates that each T pulse is completely ineffective.

The effectiveness ratio scales the degree to which the substrate has recovered from refractoriness and ranges from 0 to 1. No effect of the T pulse is described by a value of 0 and maximum effect of the T pulse is described by a value of 1. Intermediate values reflect proportional effects of the T pulse relative to the C pulse.

Significance of behavioral data. For several reasons it is thought that the behaviorally derived

refractory period data mirror the excitability properties of the axons beneath the electrode tip rather than the properties of neurons that receive synaptic input from the directly stimulated cells. First, the curves exhibit features that are reminiscent of relative refractory periods and supernormal periods (Yeomans, 1979). Second, the early part of the curve may be influenced by changes in pulse-pair interval as little as 0.1 msec; it is unlikely that synapses could be faithful to such precise temporal information. Third, the entrainment phenomenon (Kocsis, Swadlow, Waxman, & Brill, 1979) suggests that axonal properties are being measured. During the relative and supernormal periods, impulses undergo decreases and increases in conduction velocity respectively. In sufficiently long axons, the interspike interval during propagation becomes entrained to a constant interval and no longer resembles the original C-T interval. Fourth, the behavioral data are in good agreement with the electrophysiological determination of excitability cycles recorded at brain stimulation reward sites (Shizgal et al., 1982). Taken together, the above points favor the proposal that the behaviorally derived curves express the membrane characteristics of the directly activated substrate. In addition, the refractory period experiments illustrate the plausibility of the psychophysical approach and offer credibility to the trade-off functions relating other physiological properties.

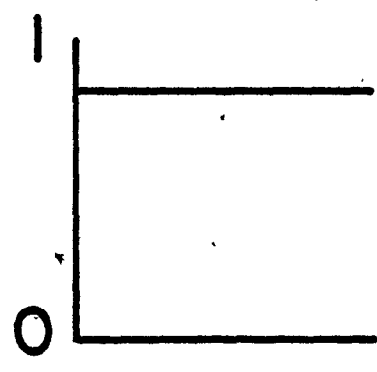
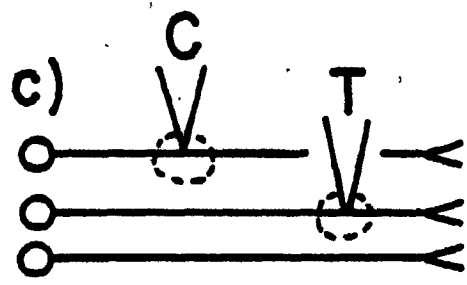
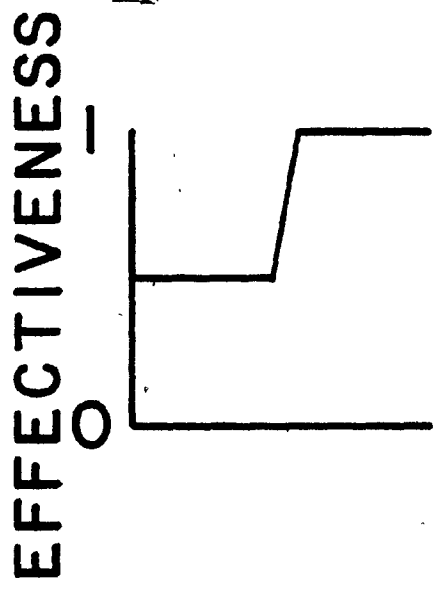
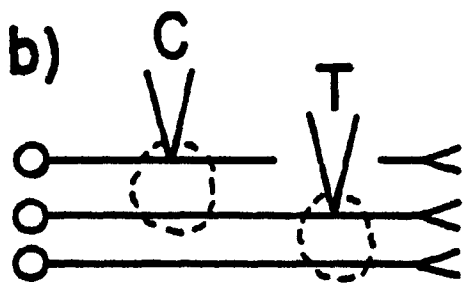
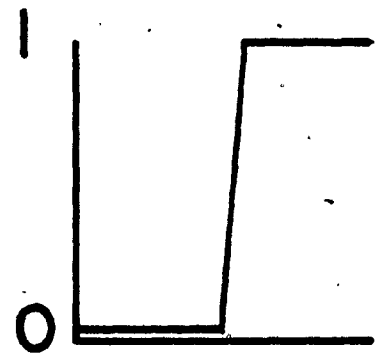
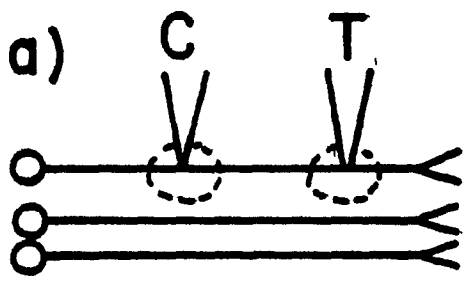
Behavioral inference of anatomical linkage and conduction velocity

As stated earlier, the direction experiment (Experiment 3) in this thesis required subjects with two electrodes that activated the same set of reward-related fibers. Accordingly, the first experiment made use of a procedure for drawing such anatomical inferences. The technique is based on the conduction failure caused by the collision of orthodromic and antidromic action potentials in an axon. It is routinely used in electrophysiological recording experiments to determine if the responses recorded in the region of the soma arise from direct stimulation of the axon originating in that soma. Lucas (1913) first used the collision procedure to determine the effect of alcohol on the conduction velocity of a known bundle of fibers. His experiment was similar to the refractory period experiment in the nerve-muscle preparation described above except that instead of delivering both C and T pulses to one electrode, the pair of pulses was split between two electrodes and the shortest interval between pulses sufficient to elicit a muscular contraction was measured. At short C-T intervals, the orthodromic impulse generated at the electrode distal to the muscle was cancelled by the arrival of the antidromic impulse arising from the proximal site. Only the orthodromic impulse generated at the electrode closest to the muscle

propagated without failure. A muscle contraction was observed when the C-T interval was sufficiently long to permit both orthodromic impulses to conduct to the muscle. This occurred when the C-T interval exceeded the sum of the conduction time between the two electrodes and the refractory period. In this manner, Lucas (1917) was able to infer the conduction velocity of the nerve segment between the two electrodes.

In brain-stimulation reward studies, the collision technique has been used differently. Shizgal et al. (1980) reasoned that one could use the collision phenomenon to assess the trajectory of fibers responsible for the rewarding effect. Like Lucas's (1917) procedure, pairs of pulses were delivered in alternating fashion to the ipsilateral LH and VTA electrodes. The effectiveness of double-pulse stimulation was assessed by comparing the number of pulse pairs required to maintain criterial responding to the required number of single pulses delivered via either electrode. The logic underlying the scaling was developed in refractory period experiments and is described earlier. Figure 2 illustrates the trade-off functions predicted from different anatomical arrangements; each axon represents a bundle of fibers. In the top panel (Figure 2a), the electrode tips are positioned at separate points along the same fibers; this is similar to the situation in Lucas's experiment. At short delays between C and T pulses,

Figure 2: Relationship between alignment of stimulation fields and collision profiles. The difference in effectiveness values between short and long C-T delays is dependent on the degree to which the fields overlap. Figure 2a represents perfect overlap, Figure 2b represents partial overlap, and Figure 2c represents no overlap.



C-T INTERVAL

collisions will occur between the orthodromic impulses from the electrode receiving C pulses and the antidromic impulses from the electrode receiving T pulses. As a result only the orthodromic volley triggered by the T pulse will reach the synapses. As the delay is lengthened to exceed the sum of the conduction time between the C and T electrodes and the refractory period of the fibers under the T electrode, two volleys reach the synaptic terminals. The curve reflecting collision effects is drawn on the right side of Figure 2a. At short C-T intervals, the effectiveness of double-pulse stimulation is zero, indicating that single and double pulses have equivalent behavioral effects. The abrupt and maintained rise in effectiveness that occurs at longer C-T intervals indicates that double-pulse stimulation is twice as effective as single-pulse stimulation. The delay at which the effectiveness scores increase, referred to as the collision interval, is interpreted as the sum of the interelectrode time and the refractory period. Division of the difference between the conduction time and refractory period into the interelectrode distance yields an estimate of the conduction velocity.

What are the grounds for interpreting the abrupt change in effectiveness as recovery from a collision block? First, the C-T intervals at which recovery from collision begins is much later than the earliest recovery associated with refractory period curves in rewarding MFB sites.

Second, local potential summation, a phenomenon typically observed at short C-T intervals in refractory period data is not apparent in collision profiles. Both findings argue against the possibility that refractory periods, rather than collision intervals, are responsible for the abrupt rise in the double-electrode data. Third, the abrupt rise occurs at the same C-T interval regardless of which electrode receives the first pulse, as expected from the bidirectional character of axonal propagation. This result is not anticipated from stimulation through electrodes in synaptically linked pathways.

Finally, in subjects demonstrating clear collision-like effects, a reduction in the stimulation currents and hence, in the size of the stimulation fields, abolishes the sharp increase in effectiveness values, yielding a flat trade-off function (Shizgal et al., 1980). This suggests that the collision effect is determined by the alignment of the electrodes in the fiber bundle. The probability that the same fibers are stimulated by both electrodes decreases with the size of the stimulation fields. Because one of the key manipulations in the direction test is related to this point, the relationship between collision effects and field size is explained in detail below.

Figure 2a depicts the ideal situation in which all stimulated elements are common to both electrodes. In

practice, the data obtained in collision studies suggest that only a proportion of the stimulated fibers are fired by both electrodes. This conclusion is based on the observation that effectiveness values for brief delays are always greater than zero. If the same population were excited by each stimulation field, collisions of anti- and orthodromic impulses would occur in all members for short C-T intervals. This does not appear to be the case. Preceding the increase in effectiveness values, the curves typically range from 0.4 to 0.7 across subjects, suggesting that there are fibers not shared by both stimulation fields and, hence, not subject to collision effects. An example of this is shown in Figure 2b. Only the middle of the bundle is common to each field; since collisions can only occur in this fraction of the pathway, the curve relating the effectiveness of stimulation to pulse-pair interval is represented by a smaller difference in effectiveness values between short and long delays. Because of the misalignment of the electrodes, no fibers that traverse both fields will be stimulated if the LH and VTA currents are decreased sufficiently. Figure 2c illustrates this point. Paired pulses delivered to electrodes located in nonoverlapping portions of the same fiber bundle yield the function to the right of Figure 1c. Effectiveness values remain constant through a wide range of delays, as the impulses elicited by the two electrodes fail to collide.

This technique has now been used to assess the trajectories of reward fibers coursing through several brain-stimulation reward sites (Bielajew et al., 1982; Bielajew & Shizgal, 1980; Bielajew & Shizgal, 1982; Silva et al., 1982; Durivage & Miliaressis, 1983; Schenk & Shizgal, 1982; Shizgal et al., 1980) and to dissociate reward fibers from those mediating other stimulation-produced behaviors (Bielajew & Shizgal, 1980; Durivage & Miliaressis, 1983).

In summary, the method just described is an important tool in the psychophysical characterization of the substrate for brain-stimulation reward. Aside from determining whether the two electrodes excite the same first-stage neurons, the collision data provide estimates of conduction velocity. Since this property is strongly correlated with fiber diameter (Swadlow & Waxman, 1978), the caliber of the first-stage reward fibers is estimated.

However, the collision technique cannot detect the normal direction of conduction in these fibers because of the bidirectional character of axonal propagation. Referring to Figure 2a,b, whether electrode C or T is driven first does not alter the time course of the collision interval. In either case, the interelectrode conduction time and a refractory period must be exceeded before impulses triggered by both C and T pulses can conduct without failure. Ortho- and antidromic conduction time are expected to be the same; given that both electrodes stimulate a subset of the same

population, the refractory periods at each site are likely to be similar. Thus, the normal direction of propagation cannot be revealed from the results of double-pulse tests.

However, if the design of the experiment were such that one of the electrodes served to block the conduction of impulses generated at the other electrode, it would then be possible to assess the normal direction of impulse traffic. The paradigm that incorporates this procedure is discussed in the next section, and forms the basis for the third and key experiment of this thesis.

The importance of the collision experiment is in generating estimates of the conduction time of these neurons; by knowing when the action potentials pass under the downstream electrode, specific predictions may be made concerning when the anodal block should be effective. In addition, the collision experiment optimizes the conditions for the anodal block experiment by selecting those electrodes and currents that stimulate some of the same reward-related fibers.

Anodal block technique

This procedure has its roots in classical neurophysiology, originating with Pflüger's extensive analysis of direct-current stimulation of frog muscle fibers (cited in Monnier, 1970). The third of Pflüger's noted laws examined the effects of currents of different polarity,

strength and direction. Most relevant to the concerns of this thesis was the finding that muscle contraction elicited by cathodal stimulation of the motor nerve was eliminated when the anode was placed between the cathode and the muscle. It appeared that the impulses generated at the cathode were prevented from propagating past the region of the nerve under the anode. In contrast, there was no reduction of the muscle contraction when the anode and cathode positions were reversed.

Current entering a neuron from an anode diminishes excitability by hyperpolarizing the membrane. To calculate the magnitude of the hyperpolarization required to block conduction, one must take into account the safety factor of the membrane. The point is illustrated in the following example. For the sake of simplicity an electrically linear membrane with no threshold accommodation is assumed.

Suppose the resting potential of the membrane is -70 mv, the threshold for excitation is -58 mv, and the current arriving from an oncoming action potential is sufficient to depolarize the membrane to -34 mv. The safety factor refers to the ratio of the difference between the resting potential and the threshold potential and the difference between the resting potential and the potential that would be achieved passively as a result of the exit of current from an oncoming action potential.

In the normal case, an action potential would be

produced as soon as the membrane potential crossed threshold. In order to observe the value of -34 mv, the immediate area from which one is recording would have to be treated with a sodium channel blocker such as tetrodotoxin so as to prevent the triggering of an action potential. It is only in the case of such a treatment that one can observe the full passive response of the membrane to the current supplied by an oncoming action potential.

In this example, a threshold depolarization is only 12 mv (-70 mv - (-58 mv)) but the input from the oncoming action potential is sufficient to cause a 36 mv depolarization (-70 mv - (-34 mv)). Therefore the safety factor for the hypothesized axon has a value of 3. A safety factor well over 1 ensures that minor fluctuations in threshold do not impede impulse conduction.

Impulses will not conduct past a hyperpolarized region only if the degree of hyperpolarization is sufficient. Referring back to the above example, the membrane with a resting value of -70 mv would have to be hyperpolarized beyond -94 mv to block conduction since the 36 mv depolarization (-70 mv - (-34 mv)) contributed by the oncoming action potential would no longer suffice to bring the membrane to its -58 mv threshold. While only 12 mv are required to depolarize the membrane, an effective hyperpolarization block requires a 24 mv change in potential suggesting that it is relatively easier to elicit firings

than it is to prevent their polarization.

Since Pflüger's demonstration of electrotonic blockade, the anodal block method has been used frequently to prevent propagation in selective fiber populations. Differential blockade is achieved because large fibers, by virtue of their greater conduction velocity, tend to be blocked before small fibers (Accornero, Bini, Lenzi, & Manfredi, 1977). Cessation of current flow through the stimulation electrodes before the slower impulses arrive at the anode allows impulses propagating along the smaller fibers to pass through the region in which the more rapidly conducting impulses are blocked (Kuffler & Vaughn-Williams, 1953). Using variants of this procedure, myelinated axons have been distinguished from unmyelinated axons and fibers within each category have been segregated (Swett & Bourassa, 1981).

Because direct current applied for prolonged periods has deleterious effects in nerve, Kuffler and Vaughn-Williams (1953) modified the basic anodal block procedure by using relatively brief pulse durations and adjusting the distances between the cathode and anode accordingly. In dissected motor roots with the appropriate nerve and muscle attachments, they placed a recording electrode on the nerve near its entry to the muscle and a pair of stimulating electrodes further away. When the anode was proximal to the muscle, all impulses triggered by very

short pulses propagated successfully to the muscle. When the durations were adjusted to exceed the time required for impulses in even the slowest fibers to propagate from the cathode to the anode, a total failure of conduction was observed. At intermediate durations, a graded block was observed, and the magnitude of the block increased with the pulse duration. When the cathode lay between the anode and the muscles, all fibers were excited irrespective of pulse duration. In this manner, Kuffler and Vaughn-Williams (1953) were able to dissociate different groups of fibers. That is, steady increases in the pulse duration blocked conduction in fibers of increasingly smaller size.

I have described this experiment in detail because of its similarity to the design of the direction study in this thesis. In particular, this study highlights the key relationships between anodal hyperpolarization block, pulse duration, conduction velocity, position of anode and cathode, and direction of conduction. These relationships are at the root of the principal experiment reported below, Experiment 3.

The direction study in this thesis is conducted by applying anodal and cathodal currents to two electrodes positioned along a pathway in which the conduction velocity has been estimated. The collision and refractory period data, collected in the first two experiments ensure that at least a subset of the stimulated fibers are activated by

both electrodes; these experiments also provide an estimate of the interelectrode conduction time in the first-stage neurons. As in the Kuffler and Vaughn-Williams (1953) experiment, a series of pulse durations are tested. Only those durations equal to or greater than the interelectrode conduction time are expected to block conduction of orthodromic action potentials generated at the cathode when the anode is positioned proximal to the terminals. When this arrangement is reversed, the hyperpolarizing current should have no effect on the propagation of impulses to the synaptic terminals. By observing the behavioral effects of stimulation in these and specific control conditions, the direction of normal conduction in fibers linking the LH and VTA is inferred. This technique was first described by Shizgal, Bielajew, & Kiss, (1980). The next section describes the rationale for this inference and its relation to strength-duration functions.

Strength-duration functions

As stated above, a series of pulse durations is tested in the direction study. These include values below and above the interelectrode conduction time. In order to assess the effects of manipulating pulse duration, the current required to sustain criterial performance at each duration is determined. The function that relates the strength of the current to the duration of the pulses is

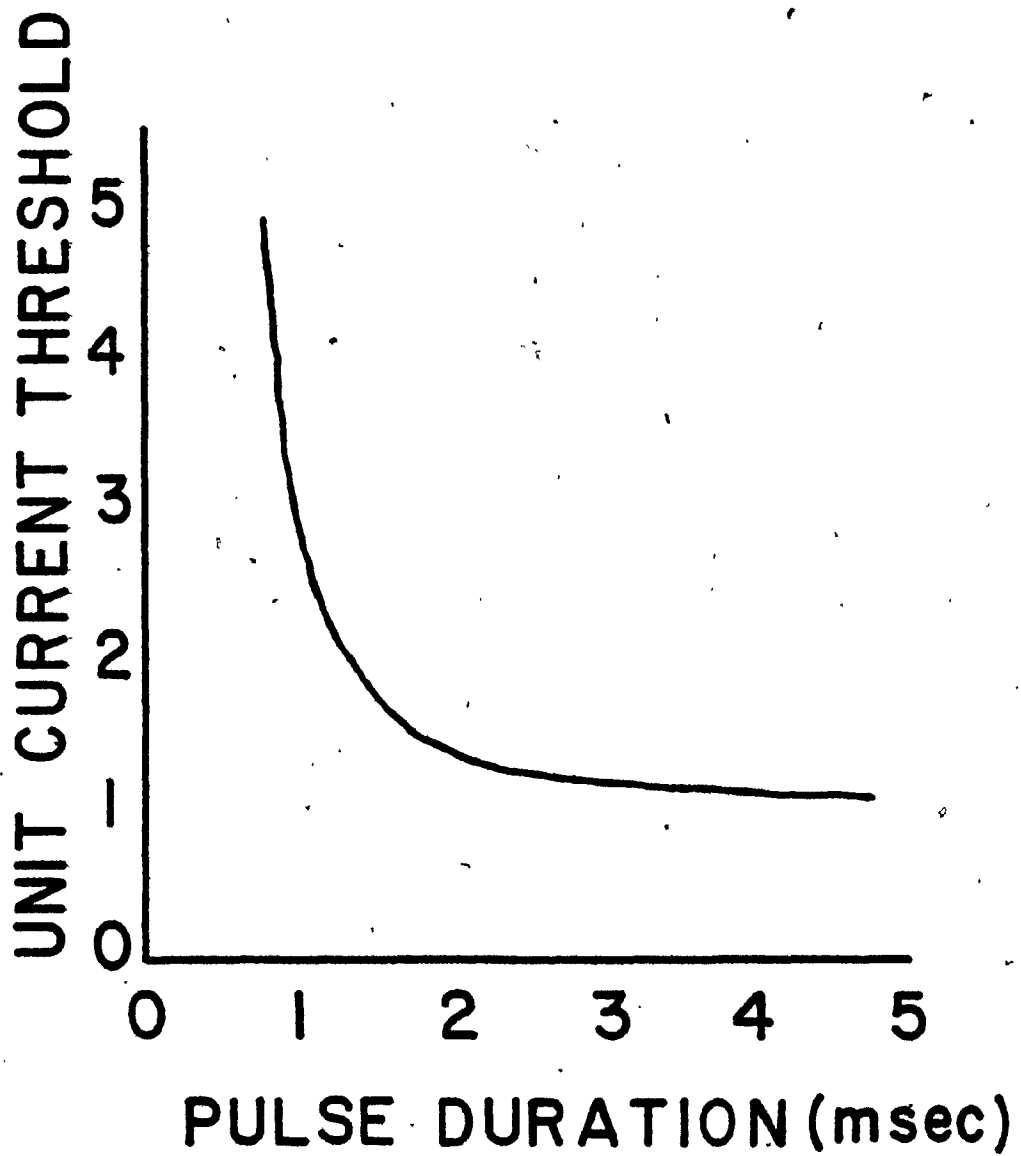
called the strength-duration function. In order to explain how direction information is gleaned from the relationship between current and duration, a brief discussion of the relevant aspects of strength-duration functions is presented below.

A typical strength-duration curve for a single cell is illustrated in Figure 3. There is initially a rapid decline in the threshold current which approaches a minimum value as duration is increased.

To understand why current and duration trade off, recall that a minimum quantity of charge must be transferred across the cell membrane in order to depolarize a cell to threshold. If a long period of time is available, a low rate of charge transfer, that is, a low current, may suffice to bring the cell membrane to threshold. If less time is available, a higher current will have to be used. Because the membrane behaves like a leaky integrator and not a perfect integrator, the quantity of charge that must be transferred to produce a given depolarization increases with the time that the current has been flowing. If the rate of charge transfer is too low, it will eventually be counterbalanced by an equal and opposite leak rate and no further depolarization will occur. This is the situation when the curve reaches rheobase.

It is traditional to describe strength-duration functions in terms of two parameters - the rheobase and the

Figure 3: Theoretical strength-duration function. The strength of the current is plotted as a function of the pulse duration.

STRENGTH - DURATION

chronaxie. The rheobase is defined as the minimum current required to elicit firings given an infinitely long pulse duration. The chronaxie corresponds to the duration at which the threshold current is twice rheobase and is believed to reflect the time course of charge integration in the membrane. The rheobase describes the scale of the function. On logarithmic coordinates, functions with different rheobases but similar chronaxies will be parallel but shifted vertically. In contrast, functions with different chronaxies and similar rheobase values will have different shapes. That is, the same horizontal asymptote will be reached but at different durations. Functions with shorter chronaxies will be more inflected than functions with longer chronaxies.

The function that best describes this curve for single units has been found to be exponential in some cases, and hyperbolic in others (Matthews, 1978). The reader is referred to Noble and Stein (1966) for an explanation of the factors that influence the shape of the strength-duration function.

Populations of neurons can also be characterized by their strength-duration properties. To understand the population function, the relationship between current, duration, and field size must be recognized. When an electrode stimulates a bundle of equally excitable cells, elements near the electrode tip will be fired by smaller

currents than cells further from the tip. As the current increases, the location at which current density is suprathreshold is pushed farther away from the tip (Ranck, 1975).

During the delivery of a stimulation pulse, cells near the tip will fire earlier than cells further from the tip. This is so because the rate at which the membrane potential changes, and hence the speed with which the threshold is attained, is dependent on the current density which in turn depends on the distance from the electrode tip. It follows from this that with current held constant, increases in duration produce concomitant increases in the size of the stimulation field. Therefore, the longer the duration the more time available for the cells in the region of low current density, the neurons distant from the tip, to reach threshold. Because both current and duration can increase field size, these parameters can be traded off. High currents and short durations have effects similar to low currents and long durations. By adjusting the pair of values, the region excited by the electrode can be held constant.

Utilization time, which refers to the time between the onset of a stimulation pulse and the triggering of an action potential, is dependent on the spatial relationship between the cell and the electrode tip. Cells close to the tip will have a shorter utilization time than cells far from

the tip. This concept has important implications for the interpretation of the third experiment.

In Experiment 3 of this thesis, the direction of normal conduction is inferred from the shape of strength-duration functions. When the anode is positioned between the cathode and the synaptic terminals, the increase in current necessary to compensate for firings lost due to conduction failure in the hyperpolarized region should force the resulting strength-duration function to decline less rapidly at long pulse durations than might be expected if the anode were positioned elsewhere. The blocked region can be imagined as a "hole" in the field; in order to replace the contents of the blocked region, neurons on the fringes of the field must be recruited. As a result, the end of the strength-duration function will be pulled up towards higher currents.

In order to compare the effects of anode location, strength-duration curves are obtained under conditions in which 1) the anode and cathode are both depth electrodes and 2) the cathode is a depth electrode and the anode is a set of skull screws.

Because the anodal block should only be effective when positioned between the cathode and the terminals, one might reason that a more expedient manner in which to assess the direction of conduction is to compare the two strength-duration functions derived from passing currents

through depth electrodes alone. When the anode is between the somata and the cathode, the impulses triggered at the cathode can propagate unhindered to the synapses. Only the function obtained from stimulating with the anode between the cathode and the synapses will be pulled up at long durations.

One reason that the comparison of strength-duration curves obtained from pairs of depth electrodes may be misleading is because the first-stage neurons activated at each site may not have identical strength-duration properties. Although the subset of elements common to each site are expected to have similar strength-duration characteristics, the remainder may not. To avoid this confound, the strength-duration curves obtained with a given depth electrode as the cathode and a second depth electrode as the anode is compared to the strength-duration curve obtained with the same depth electrode as the cathode but the skull screws as the anode. If the tip of the cathode is the only source of stimulation, then the neurons excited in these two conditions should be very similar. Moreover, the demonstration that the shape of the strength-duration function is independent of the angle of current flow suggests that the above comparison is a valid one. In the toad sartorius nerve-muscle preparation, Rushton (1927) demonstrated that the angle at which current passed through the nerve had no effect on chronaxie

measurements, although rheobase changed greatly. Thus, in the direction test, differences in the shape of the strength-duration functions obtained with a given depth electrode as the cathode and either the second depth electrode or the skull screws as the anode should not be due to the different angles of current flow. Rather, shape differences are expected to be due to the presence or absence of an anodal block between the cathode and the synaptic terminals of the first-stage neurons.

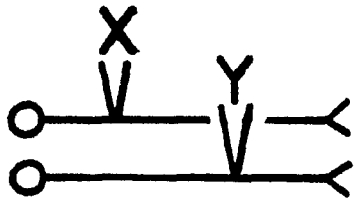
To explain how the direction of normal conduction is inferred from the shape of strength-duration functions obtained from stimulation with different electrode configurations, I will refer to Figure 4 which illustrates three examples.

By comparing the strength-duration functions obtained from stimulation with the cathode and anode as either the depth electrodes or one depth electrode and the skull screws, the examples distinguish two cases that would be confounded if strength-duration curves obtained from stimulation through depth electrodes alone were the basis of comparison. These are illustrated in Example 1 in which there is no effective block and Example 3 in which equally weighted subpopulations of ascending and descending fibers are represented.

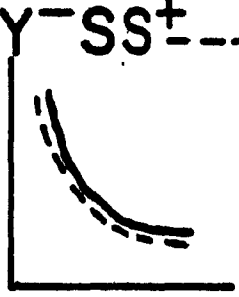
In the first example, the two electrodes are located in separate fiber bundles or in non-overlapping

Figure 4: Explanation of anode-block procedure. The relationship between the anode and the cathode positions influences the shape of the strength-duration functions. The curves on the right are grouped to illustrate the key comparison - when either two depth electrodes or one depth electrode and a skull-screw serve as the cathode and the anode.

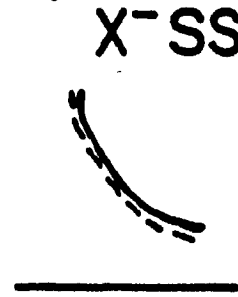
EX. 1



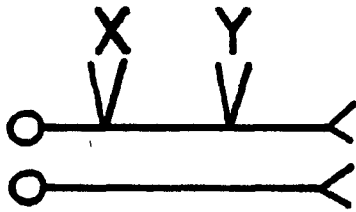
a) $Y^- X^+ \text{---}$
 $Y^- SS^+ \text{---}$



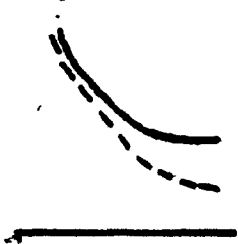
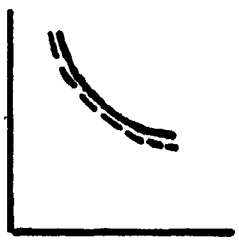
b) $X^- Y^+ \text{---}$
 $X^- SS^+ \text{---}$



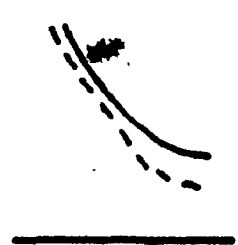
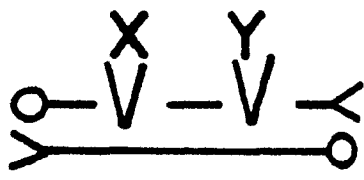
EX. 2



REQUIRED CURRENT



EX. 3



PULSE DURATION

portions of the same fiber bundle. Either arrangement should produce similar results. The graphs to the right of the drawing plot the predicted trade-off functions when different pulse durations are tested using two depth electrodes or one depth electrode and the skull screws.

Because the electrode tips in Example 1 are misaligned, the hyperpolarization block induced by one electrode should not block the impulses triggered by the other. The outcome is similar for the skull-screw condition except that the entering current, spread over a large surface area, should produce little or no block in any of the neurons. Thus, the strength-duration functions obtained in Example 1 from the stimulation conditions in which depth electrodes serve as the anode and cathode should be identical in shape to their skull-screw comparisons (Examples 1a,b).

In Example 2 both electrodes are located at different sites along the same axon bundle; the parallel curves in Figure 2a would be produced by using Y as the cathode. Even when X serves as the anode and the pulse duration exceeds the interelectrode conduction time, only the antidromic impulses generated at Y will be blocked. The orthodromic impulses will be unaffected by the anodal block at X. Hence, the number of signals that reach the relevant synapses is the same regardless of the stimulation condition; as such, parallel strength-duration functions are

expected in Example 2a.

To produce the curves in Example 2b, the positions of the cathode and anode are reversed so that the hyperpolarization occurs at Y, proximal to the terminals. At short pulse durations, the membrane potential in the region under Y will have returned to its resting value before the arrival of the orthodromic impulses from X, and a block is not predicted. Pulse durations greater than the interelectrode conduction time should reduce the number of action potentials propagating across the region hyperpolarized by electrode Y. Current entering at the skull screws should not impede conduction of orthodromic impulses triggered at X, because this current will be extremely diffuse once it has spread out to the area in which it enters the stimulated cells. Thus the shape of the strength-duration function will only be affected by the current entering at the depth electrode (Y). The curves in Example 2b should be parallel until the pulse duration approaches the interelectrode conduction time; at longer values an upward deflection should be observed in the curve. In contrast, the functions obtained from the configuration in Examples 1a, b, and 2a are expected to be parallel over their entire ranges. The direction of normal conduction will be inferred in Experiment 3 from the anode and cathode positions that obey the predictions described in Examples 1, 2, and 3 in Figure 4.

In Example 3, some orthodromic impulses will be blocked regardless of which electrode serves as the anode. As a result, the curves in Examples 3a,b will resemble the curves in Example 2a.

EXPERIMENT 1

The main purpose of this experiment was to determine if reward-related fibers directly link LH and VTA self-stimulation sites. A requirement for inclusion in the direction study (Experiment 3) was a sizeable and consistent collision-like effect. It was predicted that the direction of normal conduction would be revealed in Experiment 3 only if the current entering through the anode hyperpolarized some of the same fibers that were depolarized by the current exiting through the cathode.

Because interelectrode conduction times can be estimated by subtracting the refractory period estimates in Experiment 2 from the collision intervals obtained in this experiment, a second prediction could be tested; the direction test should yield positive results only when the duration of hyperpolarizing pulses is equal to or greater than the conduction time between electrodes. An additional aim of this study was to increase the sample of conduction velocity estimates for MFB reward fibers. It was hoped that by adding more subjects to the existing pool of ten, the conduction velocity measures would begin to cluster around a central value (Bielaiew & Shizgal, 1982; Shizgal et al., 1980):

Method

Subjects and surgery

Male hooded rats of the Long Evans strain (Canadian Breeding Farms & Laboratories) weighing from 300-450 g, were separately housed in wire-mesh or plastic cages, and maintained on a 12 hr light/dark cycle. Food and water were available freely. Prior to surgery, the animals were anaesthetized with sodium pentobarbital (60 mg/kg i.p.). Using standard stereotaxic procedures, electrodes were aimed at the ipsilateral LH and VTA. With the incisor bar set at 5.0 mm above the interaural line, the following coordinates were used: LH - 0.4 mm behind bregma, 1.7 mm lateral to the sagittal suture, and 7.5 - 8.0 mm below the dura; VTA - 3.3 mm behind bregma, 0.7 mm lateral to the sagittal suture, and 7.5 - 8.0 mm below the dura.

Electrodes were fashioned from 254 μ m stainless steel wire insulated with Formvar to within roughly 0.25 mm of the rounded tip. A fine stainless steel wire wrapped around four stainless steel anchoring screws served as the anode. The screws straddled the sagittal suture; two were located anterior to bregma and the remaining two were located near lambda. The entire assembly was secured to the skull with dental cement.

Apparatus

The test box, 25 cm wide, 25 cm deep, and 70cm high, was constructed of Plexiglas, and was fitted with a grid floor. A Lehigh Valley rodent lever protruded into the lower right corner of the left wall about 6 cm above the floor.

Stimulation consisted of 0.5 sec trains of monopolar, rectangular, cathodal pulses, 0.1 msec in duration. The temporal parameters of the stimulation were controlled by integrated circuit pulse generators and the amplitude was controlled by dual constant-current amplifiers (Mundl, 1980). In the absence of a pulse on either channel of the dual constant-current amplifier, the outputs of each channel were shorted through 1k resistors, to prevent polarization at either of the electrode tips. Stimulation parameters were continually monitored on an oscilloscope by reading the voltage drop across a 1k precision resistor in series with the rat. Periodically during a test session, the voltage drop across the rat and the precision resistor was noted, and the impedance of the electrode brain interface computed.

During testing, the animals' behavior was observed constantly; background noise was provided by CBC radio.

Procedure

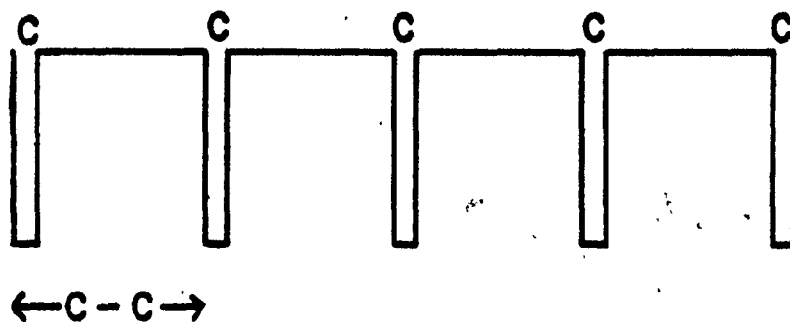
Screening and stabilization. Following a post-operative recovery period of 2-3 days, each subject was screened for self-stimulation. Animals that could not be quickly shaped to the lever for current values not greater than 400 μ A at each electrode and those that did not achieve rates of at least 30 presses per minute were discarded from the study.

Self-stimulation of each electrode site was stabilized using the following procedure. Starting with the parameters found to support high rates of responding, the current was held constant and the number of pulses was reduced by 0.1 \log_{10} steps after every trial until response rates near zero were observed. A 15 sec pause separated the 30 sec trials. This procedure was repeated until the number of pulses required to sustain a half-maximal rate of lever pressing (hereafter referred to as the "required number") did not vary by more than 0.1 \log_{10} units across five determinations. Generally three sessions were required to attain the stability criterion.

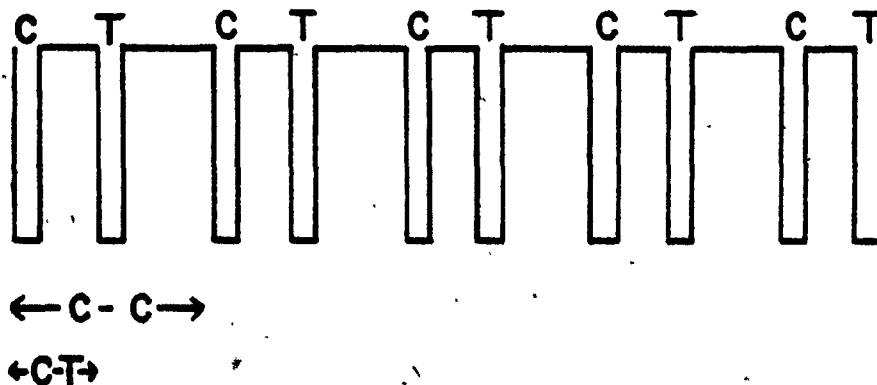
Collision test. The collision test consists of a series of determinations of the required number of single or double pulses. The relationship between a train of single and double pulses is illustrated in Figure 5. A train of single pulses in Figure 5a with a constant C-C interval (period) is converted to a train of double pulses (Figure

Figure 5: An illustration of the relationship between the single- and double-pulse conditions. (a) Trains of single pulses (C pulses) are presented. Since the train duration is always held constant, there is a reciprocal relationship between the number of pulses and the interval between pulses (C-C interval). (b) For the double-pulse condition, each C pulse is followed by a T pulse of the same amplitude.

(a) SINGLE-PULSE CONDITION
C PULSES



(b) DOUBLE-PULSE CONDITION
C & T PULSES



5b) by inserting a T pulse within each period. The C-T interval is always equal to or less than one-half the C-C interval. Each double-pulse train ends at the offset of the T pulse.

At the beginning of each session, a brief warm-up was conducted; using the intensities at which collision data were collected, the required number of single pulses was determined at each site. The experiment proper was then begun.

A typical test session consisted of a series of required-number determinations. The required number of single pulses was assessed at the beginning and end of the test as well as after every four determinations of the required number of double pulses. In the anterior-posterior test, the C pulses were delivered to the LH and the T pulses were delivered to the VTA; this order was reversed in the posterior-anterior test. About 12 C-T intervals, ranging from 0.1 to 10 msec, were tested in a random order. Each determination of the required number of double pulses was based on a different C-T interval. By repeatedly determining the required number of single pulses, it was possible to detect fatigue or sensitization effects. A session was discontinued and the stabilization procedure repeated if the required number of single pulses varied more than $0.1 \log_{10}$ units overall.

The collision tests were conducted 2-5 times per

subject and interdigitated with the refractory period tests in Experiment 2.

Pilot collision tests. The purpose of these pilot tests was to quickly predict whether the two stimulation fields were sufficiently large and well-aligned to activate some of the same reward-related fibers. These tests served to choose optimal current values and to screen out subjects in which the electrodes appeared to be too misaligned. Since the experimental procedure was extremely time consuming, an initial screening procedure was essential.

Following stabilization sessions, pilot collision tests were conducted at three pairs of LH and VTA intensity values. Two C-T intervals were tested, 0.5 and 5.0 msec. In our experience with these stimulation sites (Bielajew & Shizgal, 1982; Shizgal et al., 1980), the abrupt change in effectiveness that has been interpreted as a collision block has been observed only at C-T intervals less than 2.5 msec. If this interpretation is correct, a difference in the required-number values for short and long C-T intervals is a predictor of the existence and magnitude of the blocking effect. More pulse pairs are required at short than at long C-T intervals in order to compensate for firings lost due to collision. If, after 10 determinations of the required number at each C-T interval, there was no clear difference in the required number of double pulses, the intensity at each site was raised, performance restabilized, and the

pilot test repeated. This procedure was repeated until either a collision-like effect was observed or the compliance voltage of the constant-current stimulator was exceeded. The latter usually occurred at currents well above 1200 μ A.

Data format. The effectiveness of double-pulse stimulation was computed using the following formula (Shizgal et al., 1980):

$$E = ((RN_{SPL}/RN_{C-T}) - 1) / (RN_{SPL}/RN_{SPH})$$

where E = effectiveness of double-pulse stimulation,
 RN_{SPL} = lower of the two single-electrode
 required-number values,
 RN_{C-T} = required number of pulse pairs,
 RN_{SPH} = higher of the two single-electrode
 required number values.

This formula is equivalent to Yeomans's (1979) effectiveness equation for pulses of unequal amplitude, and was used to correct for inequalities in the required number of single pulses at each placement. The electrode yielding the higher required number contributes less to the total effectiveness of a train of double pulses than does the electrode with the lower required number. The above formula compensates for between electrode differences in the required number by

scaling the effectiveness value accordingly. When the LH and VTA yield identical required-number values, the fraction on the right reduces to 1 and the formula is the same as that used in the refractory period study (see Experiment 2).

Histology. When all experiments were completed, the animals were injected intraperitoneally with a lethal dose of sodium pentobarbital and perfused intracardially with physiological saline followed by 10% formalin. The heads were removed and placed in a stereotaxic in order to remove the electrode assembly. This was done by carefully drilling through the bone surrounding the dental acrylic cap which could then be easily lifted off the skull without disturbing the electrode tips. The distance between the tips was measured with a micrometer.

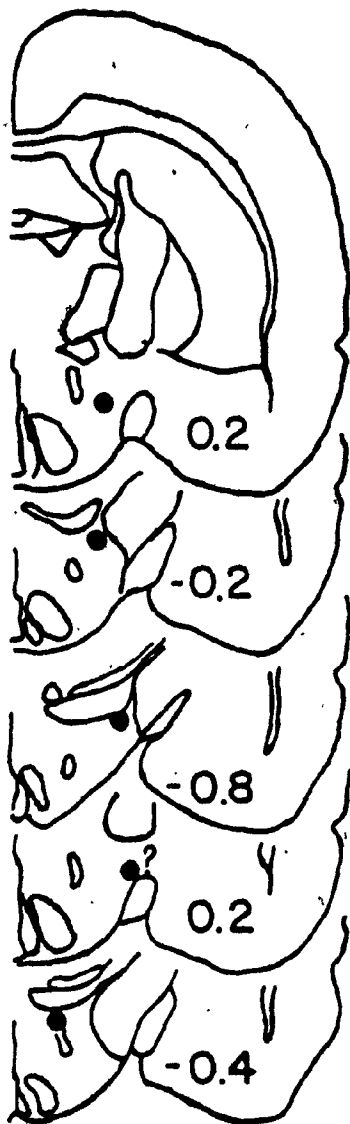
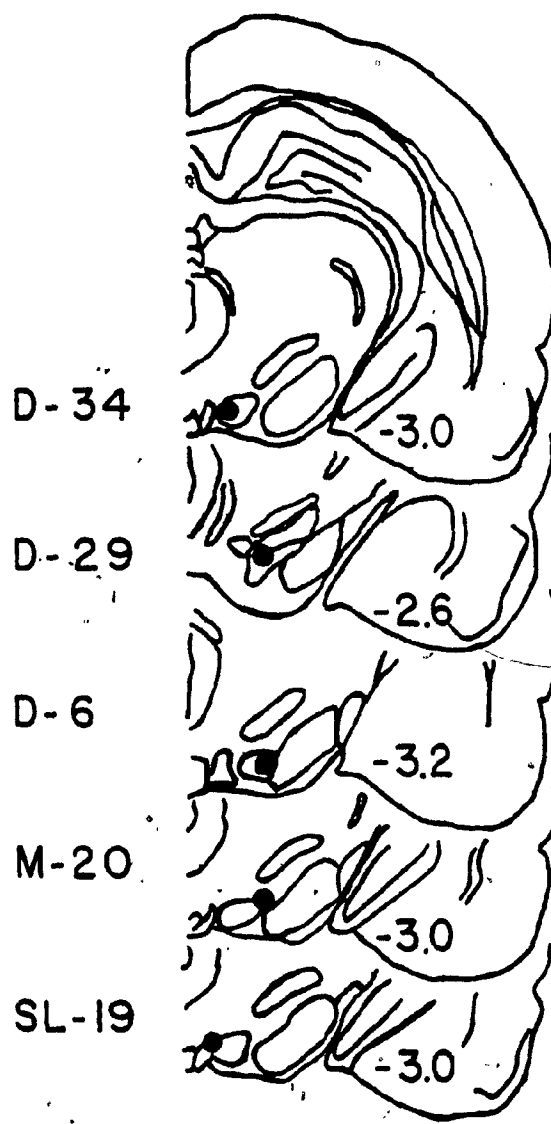
The brains were removed from the skull and placed in 10% formalin for at least 24 hr. They were then frozen and sliced into 40 μ m sections that were later stained with thionin. The Pellegrino, Pellegrino, and Cushman (1981) atlas was used as a reference in locating the electrode tips.

Results and Discussion

Histology

The location of the electrode tips is shown in Figure 6 with the anterior placements on the left and the

Figure 6: Tracing of pertinent sections from the Pellegrino et al. (1979) atlas. The filled circles indicate the location of the electrode tips. The atlas plate numbers appearing at the top of each section refer to the distance (mm) of the section from bregma. The alphanumeric located between each pair of sections refers to the identity of the subject. The anterior and posterior placements are to the left and right of the subjects respectively.

ANTERIOR
PLACEMENTSPOSTERIOR
PLACEMENTS

posterior placements on the right. The drawings are tracings of the atlas plates (Pellegrino et al., 1981) that best correspond to the sections containing the electrode tip tracks. Histology is not available for subject D-2. All anterior and posterior placements were found to be in the LH and VTA respectively. The VTA electrodes appeared to be clustered just rostral to the intended target while the anterior electrodes were scattered widely throughout the LH. The electrode tips in SL-19 deviated most from the remaining placements with respect to the mediolateral plane; both electrode tips lay closer to the midline. A question mark is set beside the anterior placement of M-20 due to uncertainty as to the position of that electrode tip.

Pilot collision data

Of the 65 animals prepared for this study, 30 passed the initial screening criteria for inclusion in the experiment. Of these, only five demonstrated a clear collision-like effect in pilot testing. With one exception (SL-19), subjects that failed to demonstrate collision-like effects were excluded from the remainder of the experiment.

In all but one case (D-29), the intensities required to observe a collision effect were rather high, (see Table 1) at least in the LH, suggesting that the failure to observe collision at lower intensities was due to a misalignment of the electrodes in the bundle of

Table 1
Summary of results from Experiment 1

Subject	LH Current	VTA Current	Interelectrode Distance	Collision Interval	Refractory Period	Interelectrode Conduction Time	Conduction Velocity
D-34	1260 μ A	630 μ A	2.8 mm	1.6 msec	0.6 msec	1.0 msec	2.8 m/sec
D-34	795 μ A	500 μ A	2.8 mm				
D-29	630 μ A	630 μ A	2.6 mm	1.2 msec	0.6 msec	0.6 msec	4.3 m/sec
D-29	450 μ A	450 μ A	2.6 mm				
D-6	1400 μ A	800 μ A	2.8 mm	1.8 msec	0.4 msec	1.4 msec	2.0 m/sec
D-6	500 μ A	355 μ A	2.8 mm				
D-2	1400 μ A	315 μ A	3.13 mm*	2.75 msec	0.6 msec	2.15 msec	1.5 m/sec
M-20	795 μ A	315 μ A	3.0 mm	1.2 msec	0.4 msec	0.8 msec	3.75 m/sec
SL-19	1000 μ A	500 μ A					

* Based on distance between LH and VTA stereotaxic coordinates

reward-related fibers. In the subjects that failed the pilot collision test, the misalignment may have been too great to be corrected by raising the stimulation intensities to the limits imposed by the constant-current amplifiers.

Adjustment of the coordinates may improve the low success rate. Using one fixed and one moveable electrode aimed at the LH and VTA, Durivage and Miliareisis (1983) report collision effects in 50% of their animals.

Collision data

The results of the AP and PA tests are presented in Figure 7. In three subjects (D-34, D-29, and D-6), data were obtained using two different pairs of intensities. The higher intensity results are shown in Figure 7a, c, e. For the same subjects, the lower intensity results are shown in Figure 7b, d, f. On the right side of the figure are the data from those subjects tested at only one pair of intensity values (Figure 7g, h, i).

The findings in Figure 7a, c, e, n, i, match earlier reports of collision-like effects (Bielajew & Shizgal, 1982; Shizgal et al., 1980). At a critical C-T interval, effectiveness values abruptly rise and remain constant at longer C-T intervals. The C-T interval just less than the one associated with the sudden increase in effectiveness is defined as the collision interval and is interpreted as the sum of the interelectrode conduction time.


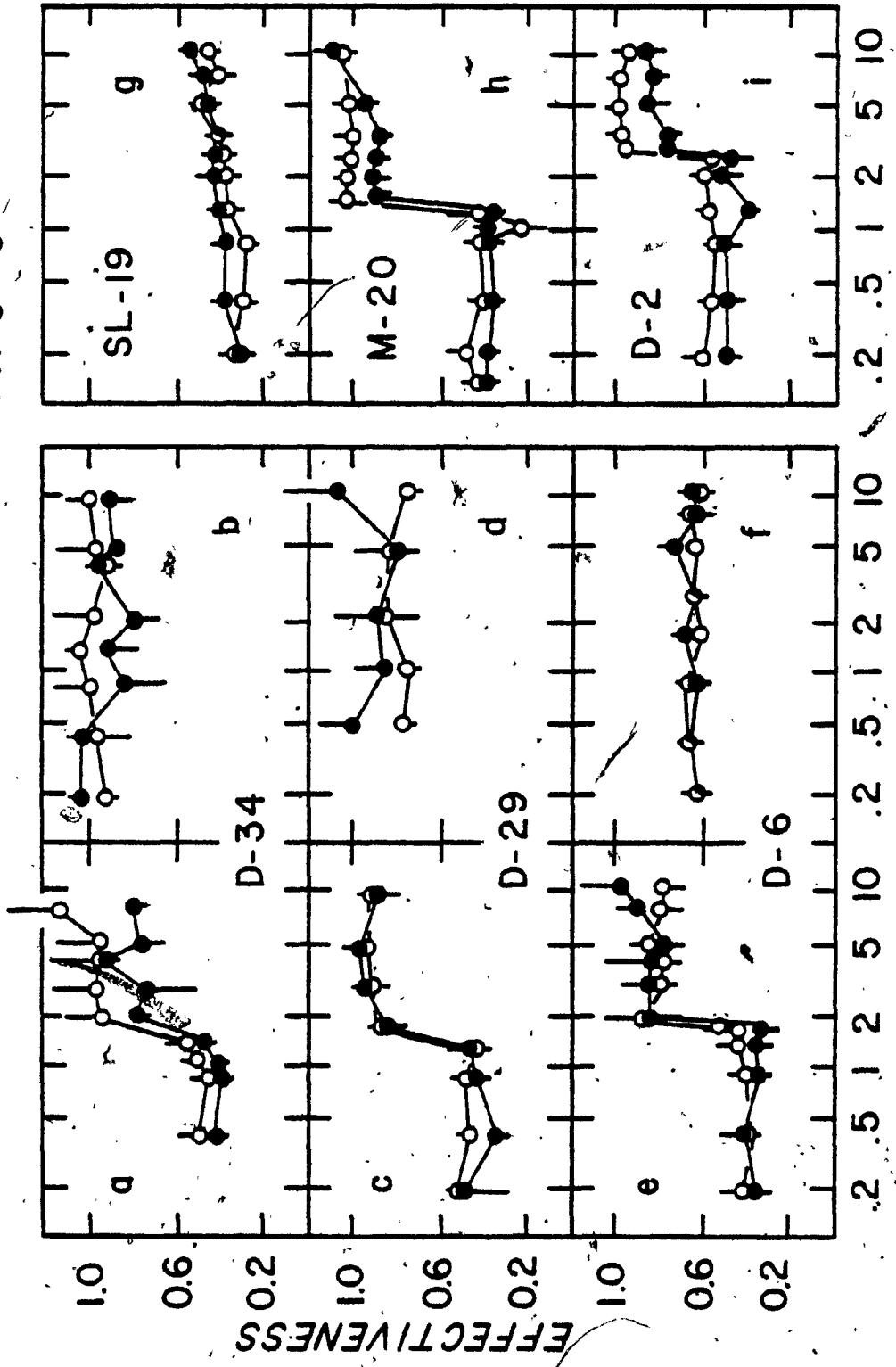


Figure 7: The results of the collision tests for each subject. The effectiveness of paired-pulse stimulation is plotted as a function of C-T interval. In the anterior-posterior condition (filled circles) the C pulse was delivered to the LH and the T pulse was delivered to the VTA; in the posterior-anterior condition (open circles) this order was reversed. The alphanumeric appearing either in the center of a pair of boxes or in the top left corner of a box identifies the subject. A pair of boxes indicates that tests were conducted at two pairs of currents. The high and low current results appear in the left and right boxes respectively.

COLLISION TESTS

AP ●—●
PA ○—○



C-T INTERVAL (msec)

and the refractory period. At these and shorter C-T intervals it appears that the conduction failure caused by the collisions of antidromic and orthodromic impulses in axons that course through both stimulation fields reduce the effectiveness of the stimulation train. When the delay between pulses is lengthened beyond these intervals, it appears that orthodromic impulses generated by each pulse propagate without interference, increasing the behavioral effectiveness of the stimulation train. The data in Figure 7a, c, e, h, i are consistent with the notion that there is overlap in the sets of reward-related fibers activated by the LH and VTA electrodes. Given the similarity of the collision profiles when the order of presentation of C and T pulses is reversed, more complicated anatomical arrangements are less likely (Shizgal et al., 1980).

In Figure 7b, d, f, the functions obtained using lower current intensities are relatively flat, showing no systematic change in effectiveness as C-T interval increases. In addition, both anterior-posterior and posterior-anterior tests yield similar results. Because increases in current intensity at the same sites produced the typical step-like profile associated with two-electrode stimulation of the same axon bundle, the simplest explanation for the flat lines in Figure 7b, d, f, is that the smaller stimulation fields were too small to activate the same reward-related fibers at both stimulation sites.

The curve in Figure 7g is an example of a case where even the largest current permissible by the stimulator failed to produce a consistent collision effect. Because an effect was observed in two of five replications and a flat line in the remaining three sessions, the average effectiveness curve in Figure 7g appears to rise steadily, a trend seen in none of the individual curves. Perhaps changes in local conditions at the electrode tips altered the shape of the LH and VTA stimulation fields across sessions.

Conduction velocity estimates

Dividing the interelectrode distance by the conduction time, the difference between the collision interval and the refractory period, yielded conduction velocity measures (refractory periods were evaluated in the second experiment).

Table 1 lists the values of current intensity for each electrode, interelectrode distance, collision interval, refractory period estimate, conduction time, and conduction velocity. Recall that conduction velocity cannot be estimated in the subjects or intensity conditions that did not yield a collision effect.

The conduction velocities computed from five subjects in this study range from 1.5 to 4.3 m/sec. Two of these estimates (D-2, 1.5 m/sec and M-20, 3.75 m/sec) have been reported earlier (Bielajew & Shizgal, 1982). The new

range falls within the range previously reported, 1.0 to 7.8 m/sec. The addition of three estimates from this experiment has had little effect on the distribution. When the estimates from this study and two previous studies are pooled, the median conduction velocity estimate is 3.8 m/sec.

Since the slopes of the functions representing recovery from collision and refractoriness (see Figure 8) are not parallel, the choice of criteria for recovery in double-pulse tests influences the resulting measures of conduction velocity. The range of C-T intervals over which recovery is observed in collision tests is usually much shorter than that reported in refractory period data. As a result, the estimates of conduction velocity will depend on the choice of a criteria for recovery in the single and double-electrode tests. In this study, the estimates were based on the C-T interval just preceding recovery from collision and the minimum effectiveness value in refractory period curves. This strategy biases the conduction velocity estimates towards lower values but is consistent with the procedure used in earlier reports (Bielajew & Shizgal, 1982; Shizgal et al., 1980).

One of the chief concerns of these previous studies was to compare the behaviorally derived rates of conduction to those obtained in electrophysiological recording studies of monoaminergic neurons (Dalsass et al.,

1978; Feltz & Albe-Fessard, 1972; German et al., 1980; Guyenet & Aghajanian, 1978; Maeda & Mogenson, 1980; Takigawa & Mogenson, 1977; Yim & Mogenson, 1980). It was important for us to estimate conduction velocity in the most conservative possible manner in order to make more meaningful any differences between our behaviourally derived estimates and the low values obtained electrophysiologically. So that the values computed here could be added to the conduction velocity estimates obtained earlier, the criterion for recovery chosen by Bielajew and Shizgal (1982) and Shizgal et al. (1980) was employed. Because the conduction velocity measures are minimized by this procedure, they provide a lower limit for MFB reward neurons. Values similar to the higher estimates in Table 1 have recently been reported from another laboratory (Durivage & Miliareisis, 1983).

For purposes of the direction study, the more critical data in Table 1 are the interelectrode conduction times which range from 0.6 to 2.15 msec across subjects. These values should be related to the shortest pulse durations at which anodal block is observed. This prediction is tested in the third experiment.

EXPERIMENT 2

The collision interval obtained for each of five subjects in the first experiment is the sum of the interelectrode conduction time and the refractory period. Experiment 2 was designed primarily to provide a within-subject estimate of the latter so that individual interelectrode conduction times could be computed and used to predict the onset of the hyperpolarization block in the third experiment. A second objective was to obtain individual estimates of recovery from refractoriness in MFB reward neurons, especially at the level of the VTA; while the refractory periods of neurons involved in self-stimulation of the LH have been well documented (Bielajew et al., 1982; Rompré & Miliaressis, 1980; Schenk & Shizgal, 1982; Yeomans, 1975; 1979), relatively few VTA placements have been examined in this respect (Bielajew et al., 1982; Bielajew & Shizgal, 1982). Finally, the design of the experiment was such that the dependence of the recovery curves on current and on the level of the MFB at which the electrode tip lay could be assessed.

The reader interested mainly in the findings related to the direction experiment (Experiment 3) can skip all of the method section after Data Format and all of the Results and Discussion section after Refractory Period Data.

Method

Subjects

The subjects and currents were the same as in Experiment 1.

Procedure

The procedure was analogous to that employed in Experiment 1 except that in the double-pulse conditions, both pulses were delivered to the same electrode. Refractory period tests were conducted at both high and low currents in subjects D-34 and D-6, the pairs of LH and VTA currents were the same as those employed in Experiment 1. In the case of D-29, the lower pair of intensities (LH-450 μ A, VTA-450 μ A) was not tested in this paradigm. The LH and VTA refractory period tests were interdigitated with the anterior-posterior and posterior-anterior collision tests and were replicated 2-5 times across subjects.

Data format. The effectiveness of the T pulse was assessed by the following formula (Yeomans, 1975) to which the formula used in the first experiment reduces when equal sized pulses are applied to a single electrode:

$$E = (RN_{sp} / RN_{C-T}) - 1$$

where E = the effectiveness of the T pulses,

RN_{Sp} = the session average of the required number of single pulses,

RN_{C-T} = the required number of double-pulse pairs for a given C-T interval.

Data analysis-asymptote test. The effectiveness values were plotted as a function of C-T interval. At short pulse-pair intervals, effectiveness values generally decline due to decay of local potential summation (Yeomans et al., 1979); at MFB placements a minimum is reached at about 0.4 to 0.6 msec. There is a gradual increase in effectiveness at pulse-pair intervals beyond these values usually reaching 80% of resting levels or more. Smaller, more gradual increases in effectiveness are sometimes seen at longer delays.

Because recovery from refractoriness tends to be gradual with no abrupt end, a visual assessment of the time course of recovery is not ideal. Consequently, a rule of thumb was devised so as to provide a consistent procedure for estimating the time course of recovery. The point after which little or no increase in effectiveness can be detected by this test is assumed to correspond to complete recovery from refractoriness. Hereafter, this test will be referred to as the asymptote test.

The assumption underlying the test is that recovery from refractoriness is complete when the curves stabilize at a plateau beyond which little change in the

curve is observed. The test starts at the longest C-T interval to contribute to the plateau and moves towards shorter C-T intervals until a point is detected at which the recovery curve slopes downward. This point is defined as the end of the refractory period.

The test is performed as follows: If the standard error about the mean effectiveness value associated with the longest C-T interval overlaps the standard error about the mean effectiveness value for the next shortest C-T intervals, all values that contribute to the two means are pooled, and a new mean and standard error are computed. The new standard error is then compared to the standard error about the next shortest C-T interval. If they overlap, the procedure of pooling and comparing is continued until a standard error about the mean effectiveness value associated with a particular C-T interval fails to overlap the standard error about the mean of the pooled values. This value is considered to be below the plateau and the next longest C-T interval is defined as the end of the refractory period.

Data analysis-transformation procedure. As stated earlier, one purpose of this study was to determine if there are differences in the time course of recovery from refractoriness both within and across stimulation sites. However, because the slope of recovery functions can be influenced by local potential summation and by what appear to be problems with the scaling method, it was necessary to

first normalize the curves before worthwhile comparisons could be made.

The factors that affect the shape of the refractory period curves include the amount of local potential summation and the asymptote or maximum effectiveness value. A substantial local potential summation contribution forces a curve to begin its ascent at effectiveness values greater than 0; this is likely due to incomplete decay of local potentials at C-T intervals corresponding to the end of the absolute refractory period of all relevant neurons (Yeomans et al., 1979). A peculiar and not understood characteristic of the curves obtained at MFB sites is that they often level off at effectiveness values much less than 1.0, thereby reducing the slope of the curve. Thus, even though the rising portions of two curves may begin and end at the same C-T intervals, the curve with no local potential summation contribution and a maximum effectiveness value close to 1.0 will have a steeper slope than a curve with a large local potential summation effect and a maximum effectiveness value well below 1.0. The transformation procedure outlined below (Bielajew et al., 1981) is designed to cancel these effects by forcing the recovery curves to span effectiveness values between 0 and 1. Only the rising portion of the curve is subject to transformation; the C-T interval corresponding to the minimum effectiveness value and the C-T interval at which

the curve approaches asymptote (as determined by the asymptote test) comprise the upper and lower bounds of the transformed portion. The effectiveness values associated with C-T intervals falling on the line forming the rising portion were transformed by the formula:

$$E_{\text{transformed}} = (E_{\text{C-T}} - E_{\text{min}}) / (E_{\text{asymptote}} - E_{\text{min}})$$

where $E_{\text{transformed}}$ = T-pulse effectiveness values adjusted to span E values between 0 and 1,

$E_{\text{C-T}}$ = the E value before transformation for a given C-T interval,

E_{min} = the lowest E value obtained,

$E_{\text{asymptote}}$ = the maximum E value corresponding to the C-T interval at which the curve approaches asymptote.

One problem with this procedure is that it excludes the contribution, if any, of neurons with very short refractory periods, that is, those that begin to recover before minimum effectiveness values are observed. The results of previous experiments (Yeomans et al., 1979) predict that this error will be small.

Results and Discussion

I. Refractory period data

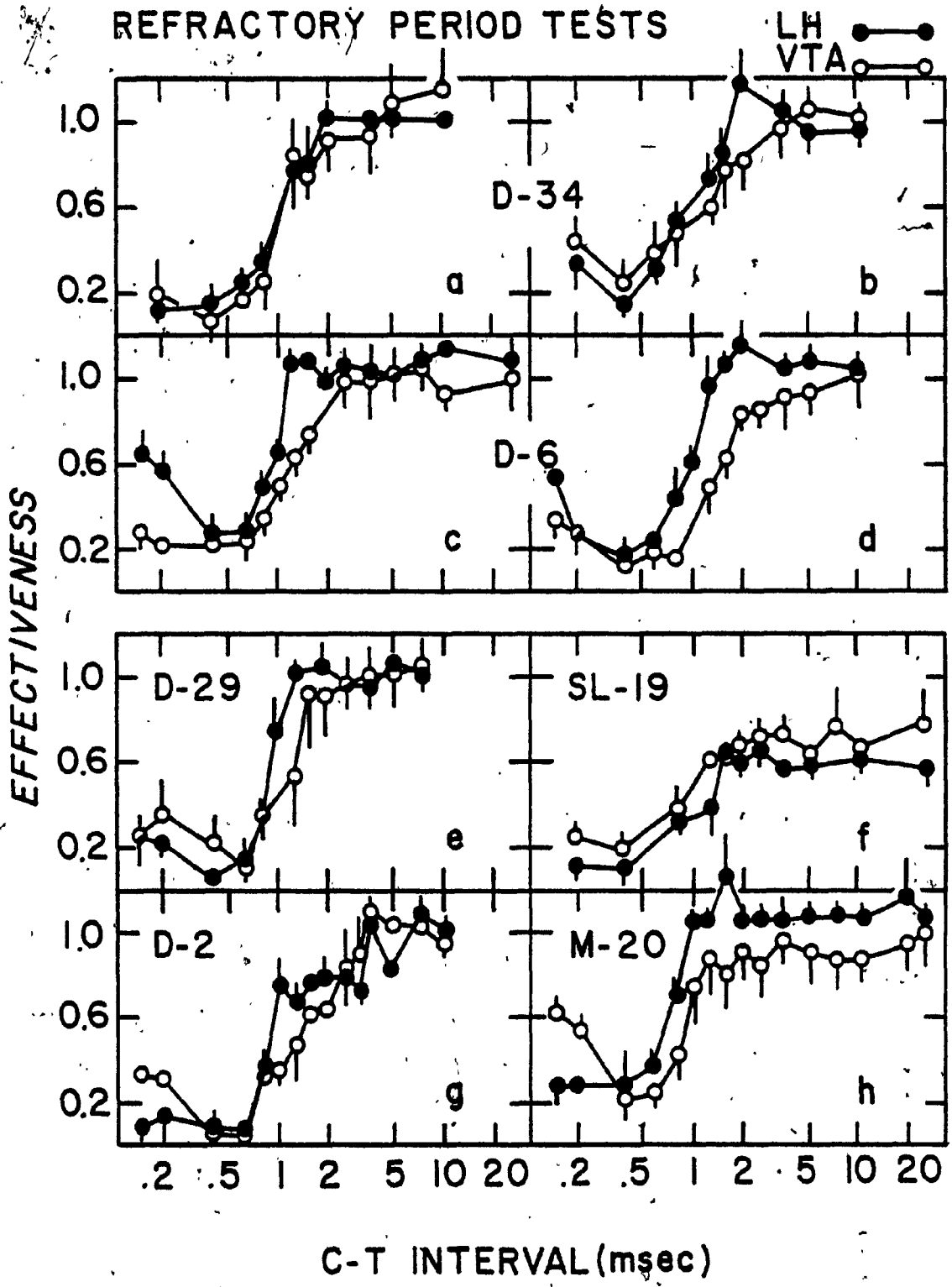
The untransformed refractory period results appear in Figure 8. The top half of the figure (a-d) represents the LH and VTA profiles for the subjects tested at two intensity values; the bottom half (e-h) represents the LH and VTA profiles for the remaining subjects in which each electrode was tested at a single intensity.

The behaviorally derived refractory period functions resemble axonal excitability changes. In most cases, local potential summation contributions are evident at the shortest C-T intervals (0.15 and 0.2 msec); at slightly longer durations (0.4 and 0.6 msec), the near 0 effectiveness values suggest that all reward-related neurons within the effective stimulation field are refractory to the T pulse. Thereafter, effectiveness values gradually increase and begin to level off at C-T intervals between 1.0 and 3.5 msec. At the longest C-T intervals, there is a suggestion of additional recovery in only one case, high intensity stimulation of the VTA site in rat D-34 (Figure 8a).

The main purpose of the study was to obtain interelectrode conduction times for each subject in order to determine the minimum pulse duration likely to produce an effective hyperpolarization block. The estimate of refractory period that contributed to the computation of

Figure 8: The results of the refractory period tests from each subject and placement. The effectiveness of T pulse stimulation is plotted as a function of C-T interval. LH results are represented by filled circles; VTA results are represented by open circles. The alphanumeric in the center of each pair of boxes or in the left top corner of a box identifies the subject. A pair of boxes for a given subject indicates that tests were conducted at different currents with high current data on the left and low current data on the right.

REFRACTORY PERIOD TESTS



conduction times was based on the C-T interval associated with the minimum effectiveness value. (The decision to use estimates that reflect the contribution of neurons with the shortest refractory periods was explained in the description of Experiment 1.) Table 2 lists the C-T interval at which effectiveness values were at a minimum at each placement and intensity value. In cases where there was a discrepancy between the LH and VTA refractory period values, the larger of the two was used to compute the interelectrode conduction time. This decision was based on the assumption that the stimulated segments of neurons that course through both effective stimulation fields and contribute to the collision effect have similar refractory periods. If a shorter refractory period estimate is obtained at one of the stimulation sites, then it is possible that the subpopulation responsible for this value is not common to both placements and hence its characteristics should not be used in the assessment of interelectrode conduction time.

II. Across-placement comparisons

Statistical analysis - asymptote test. The C-T interval at which the recovery curves approach asymptote are listed in Table 3. Note that for subjects D-34 and β -6, values were estimated for each current at which refractory period data were collected.

Of the eight comparisons that can be made across

Table 2

C-T interval (msec) corresponding to the minimum effectiveness value at each stimulation site

Subject	LH	VTA
D-34, high current	0.2	0.4
D-34, low current	0.4	0.4
D-6, high current	0.4	0.4
D-6, low current	0.4	0.4
D-29	0.4	0.6
D-2	0.6	0.6
M-20	0.2	0.4
SL-19	0.4	0.4

Table 3

C-T interval (msec) corresponding to asymptote at each stimulation site

Subject	LH	VTA
D-34, high current	1.5	2.0
D-34, low current	2.0	3.5
D-6, high current	1.2	2.0
D-6, low current	1.2	2.5
D-29	1.2	1.5
D-2	3.5	2.5
M-20	1.0	1.0
SL-19	1.5	2.0

placements, only in the case of D-2 does the LH value exceed the VTA value. In the remaining cases, except for M-20, the C-T interval at which the LH curve approaches asymptote is considerably shorter than the value for the VTA curve. The two estimates are the same in the case of M-20. Given that the LH and VTA curves begin to rise at similar C-T intervals, the rate of recovery from refractoriness at the VTA site appears to be somewhat lower. This impression was confirmed by statistical tests described below.

At least two explanations may account for this phenomenon. The later recovery at the VTA site may reflect the contribution of subpopulations of reward neurons with long absolute refractory periods that are not present at the LH site. Alternatively, the VTA substrate may include neurons with greater relative refractory periods. Using Yeomans's (1979) unequal pulse technique to distinguish between the contributions of absolute and relative refractory periods to the recovery curves, Bielajew et al. (1982) found substantial relative refractory period contributions only in MFB neurons that continue to recover beyond C-T intervals of 1.2 to 1.5 msec. In this study, the LH recovery profiles are near asymptote at these durations (median C-T interval at which asymptote is approached: 1.3 msec), while the VTA curves begin to level off later (median = 1.9 msec). The results of the earlier unequal pulse study suggest that relative refractory period contributions might

account for the slower recovery at the VTA site in this experiment.

It is interesting to note that in the animals tested at two pairs of intensities, the difference between the C-T intervals at which the LH and VTA curves approach asymptote is greatest at those intensities that failed to yield a collision effect. This finding is consistent with the interpretation that the collision effect occurs in axons common to both stimulation fields. It is thus more likely that there would be a greater similarity in refractory period estimates obtained with currents that stimulate some of the same neurons at both sites.

Statistical analysis - transformed data. A comparison of the LH and VTA refractory period data collected at each pair of intensity values is shown in Figure 9 before and after transformation. Figure 9 is the same as Figure 8 except that the transformed data have been added. For subjects D-34 and D-6, the high and low intensity data appear on the left and right sides of the graph respectively. The transformed data in all cases are to the right of the untransformed curves and are drawn on linear-linear instead of semi-logarithmic coordinates. Because of the wide range of C-T intervals tested and the events that occur at short C-T intervals, the untransformed data are more manageable on a logarithmic abscissa.

The purpose of the transformation was to make the

Figure 9: The results of the untransformed and transformed refractory period results for each subject and placement. The untransformed and transformed results appear to the left and right of the letter number combination that identifies the subject. For subjects D-34 and D-6, the high current data are located on the left side of the figure, while the low current data are located on the right side of the figure.

refractory period curves amenable to a statistical analysis of the time course of recovery. Although the C-T intervals corresponding to minimum and maximum effectiveness values suggest that refractory periods at the VTA site are longer than at the LH site, a statistical test confined to these extreme values would lack power due to the small sample in this study. Accordingly, regression tests were employed which take into account all the values that contribute to the rising portion of the LH and VTA refractory period curves. The transformation makes the regression analysis viable.

The analysis of variance approach to regression (Neter & Wasserman, 1974) was used to determine if more variance was accounted for by fitting a single line to all the data points comprising the LH and VTA recovery curves or by fitting separate regression lines to each of the two curves. The analysis was performed on the transformed data in Figure 9b, d, f, h, j, l, n, p. The limits of each curve are dictated by the minimum effectiveness values and the results of the asymptote tests for assessing maximum effectiveness values (see Tables 2 and 3).

If significant F ratios were found, the analysis proceeded to a second stage. Because differences in slope or intercept could contribute to the F ratios, a further test was carried out to determine if slope differences contributed to the significant F ratios.

The F ratios are reported in Table 4. Significant F values were obtained for the comparisons between the transformed LH and VTA curves for subjects D-34 (low intensity), D-6 (low and high intensities), and D-29. As can be seen from a visual inspection of Figure 9d, f, j, l, the curves do appear to diverge at the longer C-T intervals. Indeed, the t test results presented in Table 5 confirm this observation. Each slope difference is highly significant. Moreover, the direction of this effect is consistent, that is, the rate of recovery at the LH always surpasses the rate of recovery at the VTA site. Given that the collision experiment suggests that some of the stimulated cells are fired by both electrodes, what might explain the discrepancies in the rate of recovery at each site? A possibility is that the cells common to each stimulation field are responsible for the early portions of the refractory period curve. In fact, the data in Figure 9 and the minimum effectiveness values in Table 2 back this idea, that is, many of the curves are indistinguishable at the early C-T intervals.

III. Within-placement comparisons

Statistical analysis - asymptote test. The C-T interval corresponding to maximum recovery from refractoriness at the LH and VTA placements are listed in Table 3 for both of the currents used at each site. Only the

Table 4

Results of F tests for determining equality of regression lines for across-placement comparisons

Subject	F ratio	df	Significance Level
D-34, high current	1.156	2/42	0.325
D-34, low current	15.174	2/47	8.2×10^{-6} *
D-29	4.788	2/32	0.015*
D-6, high current	14.150	2/44	1.8×10^{-5} *
D-6, low current	18.204	2/43	1.9×10^{-6} *
D-2	0.542	2/28	0.588
M-20	2.843	2/32	0.073
SL-19	2.129	2/24	0.141

*significant (p .025)

Table 5

Results of significance test for LH and VTA slopes of
recovery functions

Subject	LH Slope	VTA Slope	df	+ score	Significance Level
D-34 low current	0.675	0.316	47	5.698	$3.8 \times 10^{-7} *$
D-29	1.300	0.892	32	4.340	$6.7 \times 10^{-5} *$
D-6 high current	1.276	0.650	44	10.793	$< 1.0 \times 10^{-10} *$
D-6 low current	1.099	0.499	43	11.111	$< 1.0 \times 10^{-10} *$

*Significant, p .05 (2 tail)

data from two subjects (D-34 and D-6) are relevant to this analysis. In the LH, the C-T interval corresponding to asymptotic recovery in the low intensity condition for D-34 was shorter than in the high intensity case by 0.5 msec while the C-T interval corresponding to the asymptote was the same for both conditions in D-6. The largest difference was found at the VTA site in rat D-34, with a 1.5 msec disparity in the C-T intervals at which the asymptote was approached. The surprising feature of these data is that in three of four comparisons, the C-T interval associated with near-complete recovery was longer when the current was reduced; in the fourth comparison, no difference was found between intensity conditions.

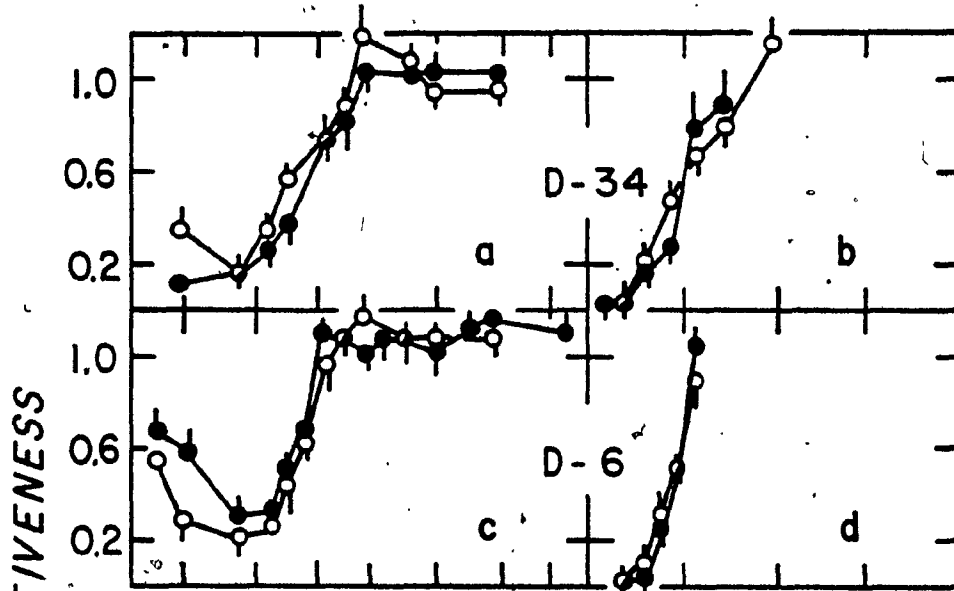
Statistical analysis - transformed data. To determine whether the differences in the rate of recovery at each intensity level were indeed significant, the analysis of variance approach to regression (Neter & Wasserman, 1974) was applied to the data from subjects D-34 and D-6. To illustrate these results, the relevant curves from Figure 9 have been regrouped to show the effects of intensity on the recovery function; the regrouped curves appear in Figure 10. As before, the transformed data are located in the right-hand panels of each box.

As might be expected from a visual inspection of Figure 10, a significant F ratio was obtained in both sets of VTA, but not LH data (see Table 6). Although the curves

Figure 10: The untransformed and transformed refractory period results regrouped to illustrate differences in current. The LH data appear above the VTA data. Filled circles represent the high current conditions; open circles represent the low current conditions. The untransformed and transformed data are located to the left and right of the alphanumeric that identifies the subject.

HIGH INTENSITY ●—●
 LOW INTENSITY ○—○

LH DATA



VTA DATA

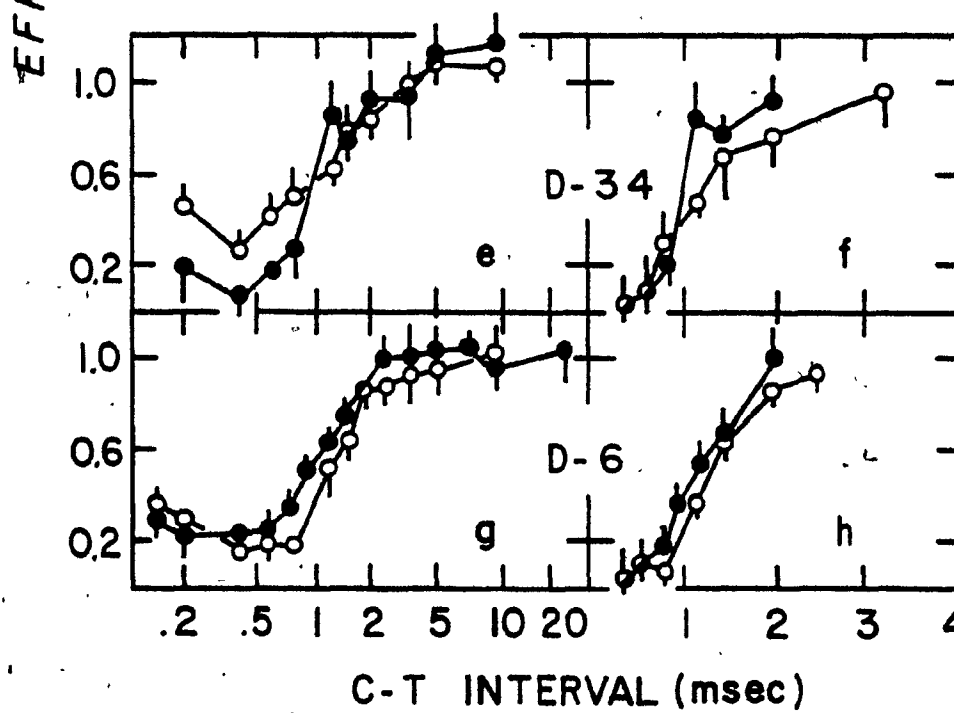


Table 6

Results of F-test for determining equality of regression lines for within-placement comparisons

Subject	Placement	F ratio	df	Significance Level
D-34	LH	1.513	2/44	0.231
D-34	VTA	4.903	2/45	0.012*
D-6	LH	0.833	2/36	0.443
D-6	VTA	4.286	2/51	0.019*

* Significant, $p < .025$

obtained at the LH placements using high and low currents approached asymptote at different C-T intervals, the F ratio did not reach significance. According to the results of the t test for slope differences, the characteristic that distinguishes the recovery curves obtained with high and low intensity stimulation of the VTA is the slope (D-34, $t_{45} = 4.197$, $p = 6.3 \times 10^{-5}$; D-6, $t_{51} = 0.019$, $p = 2.1 \times 10^{-4}$). In both D-34 and D-6, the increase in current appeared to reduce the range over which recovery from refractoriness occurred. (As discussed earlier, it is not clear whether the C-T intervals associated with recovery at either intensity reflect the major contribution of absolute or relative refractory periods.)

The finding reported here is contrary to the result reported by Yeomans and Mercouris (1983) who found increases in refractory period estimates as current is raised. It is intuitive that by virtue of their smaller diameter (Swadlow & Waxman, 1978), elements with longer refractory periods would be recruited by more intense stimuli. Hence, the C-T intervals corresponding to asymptotic recovery should have been longer in the high intensity condition. Instead, shorter values were observed. It is possible that the distribution of fibers sampled by my electrodes was such that the proportion of smaller neurons decreased as the current intensity was raised.

Finally, the ratio of cells within the absolute

and relative refractory regions of the effective stimulation fields may have changed as a function of current. Especially in the VTA, where the bundle of fibers appears to be more compact than in anterior MFB placements, (Nauta & Domesick, 1978), an increase in current might have enlarged the effective stimulation field beyond the limits of the bundle and increased the proportion of neurons subject to high current-density stimulation. If so, the rate at which recovery occurs at higher intensities would be increased in the VTA.

IV. Conclusion

The main objective of this experiment was to provide estimates of refractoriness for neurons subserving self-stimulation of the LH and VTA so that interelectrode conduction times for each subject could be computed from collision data and applied in interpreting the results of the direction experiment. The C-T interval corresponding to minimum effectiveness was the refractory period value entered in the computation; these values ranged from 0.4 to 0.6 msec across subjects. Subtraction of these estimates from collision intervals yielded the conduction time estimates; these spanned 0.6 to 2.15 msec.

Several effects unrelated to the principal aim of this experiment were observed. In half of the sample, a significant difference in the range of C-T intervals

associated with the rising portion of LH and VTA refractory period curves was found. These VTA curves required an average of 0.5 msec longer than the LH curves to attain complete recovery.

The second finding was that at least in the VTA, the range of C-T intervals corresponding to recovery depended on the current. Higher currents yielded significantly shorter refractory periods than lower currents.

In summary, these results, although rather preliminary, raise questions about the circuitry underlying brain-stimulation reward in the MFB. It appears that subtle differences in refractory period characteristics might distinguish the cells involved in self-stimulation of the LH and VTA, adding greater resolution to the criteria defining reward-related elements.

EXPERIMENT 3

Pflüger demonstrated long ago that muscle contractions produced by motor nerve stimulation could be eliminated or substantially reduced by hyperpolarizing the nerve between the stimulating electrode and the muscle. The same principle is applied in this experiment. In Pflüger's preparation, the phenomenon of anodal blockade was studied in a system in which the normal direction of propagation was known. In the present experiment, the well-known mechanisms of anodal block are used to study a pathway in which the normal direction of propagation is unknown. When the anode is between the stimulating electrode and the synapses, the hyperpolarization induced by anodal stimulation should block the conduction of signals triggered by the cathode. No behaviorally effective blockade is expected when the position of the anode and cathode is reversed.

Method

Subjects

The subjects were the same as in Experiments 1 and 2.

Stimulation conditions

The procedure consists of delivering trains of

single pulses. The electrical circuit is completed by having the current enter through an anode at one location and exit through a cathode at another location. In this design (Shizgal et al., 1980), three electrodes, two depth electrodes and the skull-screws (SS), are available as either current sinks or sources. Two basic electrode configurations are tested in the direction test. Either a depth electrode serves as the cathode and the SS as the anode or one depth electrode serves as the cathode and the other as the anode. The first arrangement is comparable to the conditions in Experiments 1 and 2. Given that either of the two depth electrodes can serve as the cathode a total of four stimulation conditions are tested. The four conditions are grouped into two pairs that form the key comparisons in the experiment. They are identified as follows. The curves obtained with the configuration $LH^- SS^+$ are compared to those obtained with the configuration $LH^- VTA^+$ as are the curves obtained with the $VTA^- SS^+$ and $VTA^- LH^+$ configurations. The negative sign indicates that the electrode served as the cathode; the positive sign indicates that the electrode served as the anode.

As explained earlier, the direction of normal propagation should be revealed by the difference in the shape of the strength-duration functions obtained using a given depth electrode as the cathode and either the other depth electrode or the skull screws as the anode.

The purpose of the collision test in Experiment 1 was to determine the sizes of the LH and VTA stimulation fields that suffice to activate a common set of reward-related fibers. In the direction test, an effective hyperpolarization block is expected only in pathways that traverse the LH and VTA stimulation fields. Consequently, it was necessary to ensure that the same cathodal stimulation fields were maintained in both experiments. This was achieved by forcing the two data sets to overlap. In the collision experiment, the current through each electrode is held constant and the pulse number is varied in order to determine the required number of single pulses. In the direction experiment, the pulse number is held constant and the current is varied in order to determine the required current. The pulse number in the strength-duration tests was set to correspond to the required number of single pulses obtained in the collision tests. For example, when a current of 795 μA was applied to the LH electrode of M-20 in Experiment 1, an average of 10 single pulses, 0.1 msec in duration, were required to support criterial responding. As expected when the $\text{LH}^- \text{SS}^+$ condition was tested in M-20 in Experiment 3, it was found that approximately 800 μA sufficed to produce criterial performance for 10, 0.1 msec pulses. If the first stage neurons are equally excitable and no firings are produced at the anode, then all pairs of currents and pulse durations on the strength-duration curves

obtained with a given cathode should excite the same region as the pair of parameters used with that cathode in collision tests. The consequences of anodal stimulation and across-cell differences in excitability are discussed below; the effects of these violations are all in the same directions, that is, they increase the effectiveness of stimulation and hence, reduce the size of the field required to support criterial performance. Thus, these violations of the assumptions should make it more difficult to measure the effect of an anodal hyperpolarization block.

In three subjects, D-34, D-29, and D-6, two different field sizes were tested with each depth electrode. Collision effects were observed only when the higher currents were used. In order to assess the effects of different field sizes in the direction experiment, two sets of parameters were employed. One set corresponded to the required number of single pulses obtained from high current stimulation at the LH and VTA (high current data). The second set corresponded to the required number of single pulses obtained from low current stimulation (low current data) at the LH and VTA. The phrases, low current data and high current data, have been employed to describe the results of the direction tests, so as to be consistent with the terminology used in Experiments 1 and 2. Thus, eight strength-duration curves, four per cathode, were collected from the subjects in which both low and high currents were

used. One pair of cathode curves was obtained with high current stimulation, the other with low current stimulation.

Procedure

The direction tests began after the collision and refractory period tests were completed. For each stimulation condition, the following procedure was employed. With the number of pulses held constant at the values obtained from Experiment 1, the current was varied from a level yielding maximum performance to a level at which there was little or no responding. The required current, defined as the current corresponding to half the maximum response rate, was computed by interpolation. The required current was determined for a series of pulse durations, ranging from 0.1 to 6.4 msec across subjects. Each subject received 2-8 tests of each stimulation condition; the conditions were tested in an interdigitated manner.

The resulting strength-duration functions were plotted on logarithmic coordinates in order to distinguish between parallel shifts and changes in shape. The functions were paired so as to highlight the critical comparisons.

Results and Discussion

The shapes of the strength-duration functions

The strength-duration curves for each subject are

drawn in Figures 11 and 12. From left to right, the three panels in each figure represent the strength-duration curves for the conditions $LH^- SS^+$ and $LH^- VTA^+$, strength-duration curves for the conditions $VTA^- SS^+$ and $VTA^- LH^+$, and the ratios of the strength-duration curves obtained with a given depth electrode as the cathode and either the second depth electrode or the skull screws as the anode. Only the high current data associated with collision-like effects are shown in Figure 11. The same arrangement is used in Figure 12 to illustrate the low current data which correspond to parameters that failed to produce collision-like effects in subjects D-6, D-29, and D-34. As well, this figure includes the strength-duration results from the one subject, SL-19, that showed no clear evidence of a collision-like effect at any currents.

Unlike the strength-duration data from the VTA^- conditions which remain nearly parallel, the LH^- curves in Figure 11 converge at the longer pulse duration. This effect is only observed in the high current data. Regardless of the anode position, the shapes of the LH^- and VTA^- strength-duration functions in Figure 12 are relatively constant at parameters corresponding to the absence of collision-like effects. Thus, the only situation in which strength-duration curves did not appear to be parallel was the one in which the $LH^- SS^+$ and $LH^- VTA^+$ configurations were tested at the range of currents corresponding to

Figure 11: The strength-duration functions obtained from the two stimulation conditions at each placement form the larger left panel of the figure. The ratio of the currents obtained at each placement form the smaller right panel of the figure. The \log_{10} intensity or intensity ratio is plotted as a function of pulse duration. The filled circles in the left panel indicate that a skull screw anode was used; in the right panel, the filled circles represent the ratio of the $LH^- VTA^+$ to $LH^- SS^+$ currents. The open circles in the left panel indicate that the second depth electrode served as the anode; in the right panel, the open circles represent the ratio of the $VTA^- LH^+$ to $VTA^- SS^+$ currents. Only data obtained at currents consistent with a collision effect are plotted in Figure 11.

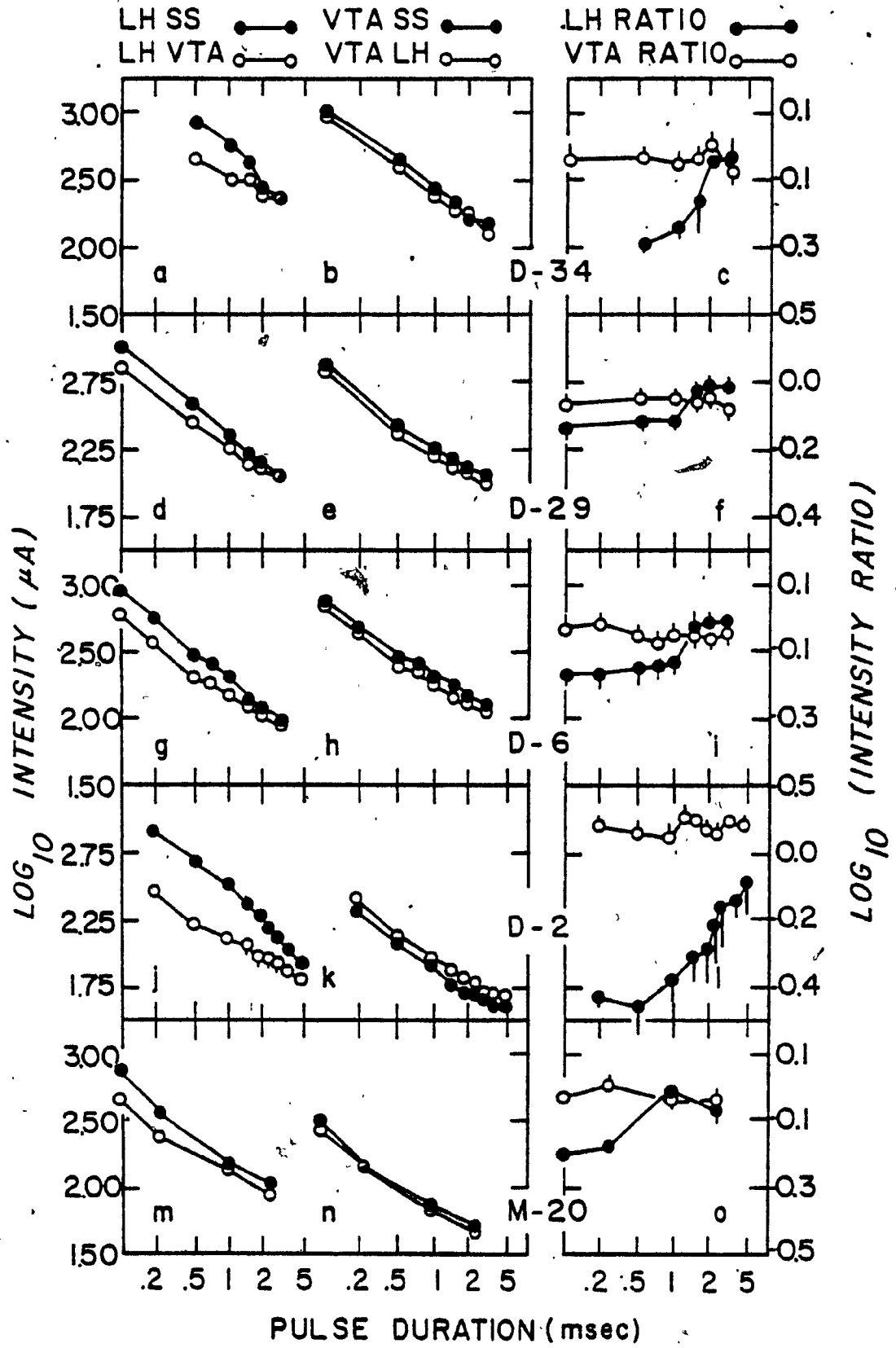
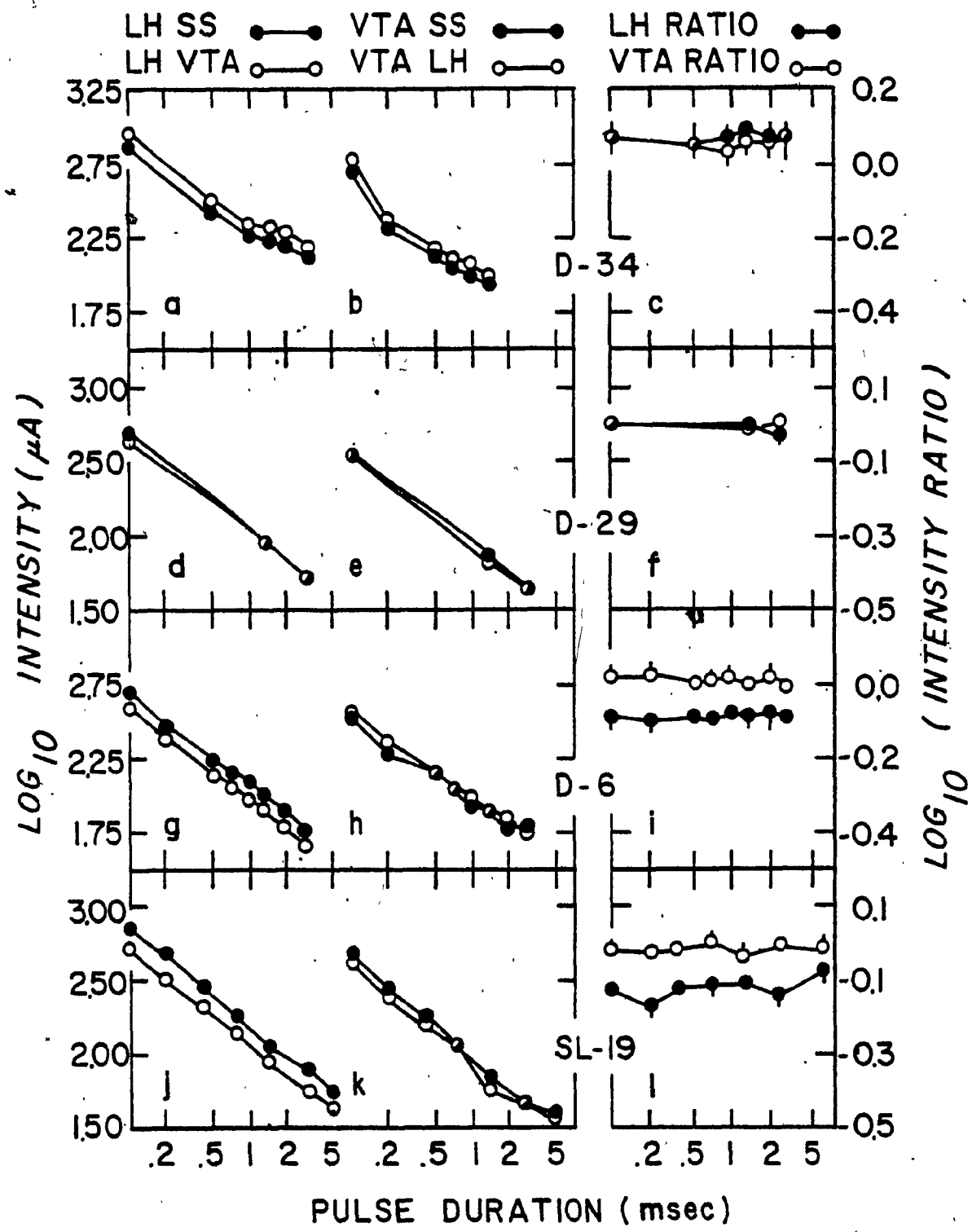


Figure 12: The strength-duration functions obtained from the two stimulation conditions at each placement form the larger left panel of the figure. The ratio of the currents obtained at each placement form the smaller right panel of the figure. The \log_{10} intensity or intensity ratio is plotted as a function of pulse duration. The filled circles in the left panel indicate that a skull screw anode was used; in the right panel, the filled circles represent the ratio of the $LH^- VTA^+$ to $LH^- SS^+$ currents. The open circles in the left panel indicate that the second depth electrode served as the anode; in the right panel, the open circles represent the ratio of the $VTA^- LH^+$ to $VTA^- SS^+$ currents. Only data obtained at currents consistent with the absence of a collision effect are plotted in Figure 12.



collision-like effects. This finding is consistent with the notion that the hyperpolarization induced at the VTA blocked the propagation of some signals generated at the LH cathode, and forced the strength-duration function to decline less steeply at pulse durations approaching or exceeding the interelectrode conduction time. Accordingly, the simplest explanation for the data in Figure 11 and 12 is that the behaviorally effective direction of conduction in the first stage is descending.

In the hypothetical examples in Figure 4, the anodal block causes the strength-duration function representing stimulation with the anode between the cathode and the terminals to diverge from the curve representing stimulation with the same cathode and a skull-screw anode. In contrast, the curves in Figure 11 that are interpreted to reflect an anodal block all converge towards the curves representing stimulation with the same cathode and a skull-screw anode. The claim that the curves in Figure 11 are all consonant with the predictions expressed in Figure 4 is based on the non-parallelism of one set of curves from Figure 11 and not on the relative position of the curves on the ordinate. If the LH⁻ curves in Figure 11 were forced to begin at the same point, then these curves would indeed diverge. The factors that alter the position of the functions on the ordinate are discussed below.

What plausible effects other than anodal block are

likely to cause the strength-duration functions obtained from $LH^- VTA^+$ stimulation at high currents to approach asymptote earlier than the curves obtained in the remaining conditions? Perhaps the angle of current flow between the two depth electrodes changes the shape of the function, despite Rushton's (1927) demonstration to the contrary. If so, one would expect a similar effect when the anode and cathode were reversed. Instead, the curve representing $VTA^- LH^+$ stimulation is parallel to the curve representing $VTA^- SS^+$ stimulation in every subject. Another possibility is that the difference in the shapes of the LH^- strength-duration functions reflects not the conduction failure of impulses triggered at the LH when the VTA is the anode but rather some peculiar characteristic of the strength-duration functions obtained with $LH^- SS^+$ stimulation. What is difficult to reconcile with this argument is the failure to observe the same shape difference in the LH^- strength-duration functions when the current is reduced. If the above proposal were correct, there would be no reason for the difference in the shape of the LH^- strength-duration functions to be dependent on current.

The demonstration in Experiment 1 that the LH and VTA stimulation fields excite some of the same first-stage neurons increases the likelihood that an anodal block could be produced when one of these electrodes served as the cathode and the other as the anode.

Hence, a better explanation of the data in Figure 11 is that some impulses triggered by the LH cathode were prevented by the VTA anode from reaching the synaptic terminals when the pulse durations approached or exceeded the interelectrode conduction time. The failure to obtain similar effects with VTA⁻ stimulation or LH⁻ and VTA⁻ stimulation at reduced currents is consistent with this interpretation.

The ratios of the strength-duration functions

The ratio data in the right panels of Figures 11 and 12 best exemplify changes in the shapes of the strength-duration functions obtained with a given cathode. If, for example, the hyperpolarization induced by the anode fails to block relevant signals, the ratio of required currents at each pulse duration would remain constant, assuming that there is no contribution of anode-make activation (see below). Thus, direction is assessed in the ratio data by noting which curve, LH⁻ or VTA⁻, is different from a horizontal line.

Only one of the ratio conditions in Figures 11 and 12 deviates from a flat line. The curves representing the ratio of required currents in the LH⁻ VTA⁺ and LH⁻ SS⁺ conditions are fairly flat at short durations and then rise at durations somewhat lower than the estimated interelectrode conduction time.

The timing of the block

Table 7 lists for each subject the interelectrode conduction time and the range of pulse durations at which the block appears to begin. The estimates in the right column of Table 7 were obtained by comparing the standard error about the current ratio associated with the shortest pulse duration to adjacent values until one was found whose standard error did not overlap the one associated with the shortest pulse duration. Because only a few, widely spaced, pulse durations were tested in some subjects (e.g., M-20), the estimates are likely to be inflated. Thus, the table lists not only the estimates obtained by the rule-of-thumb described above but also the next shortest duration. The effective blocking duration probably lies between these two values.

With the exception of D-2, there appears to be a rough correspondence between the estimated interelectrode conduction times and the estimated range of effective blocking durations. Nonetheless, effective blocking durations are generally longer than the interelectrode conduction time. This may seem surprising given that the procedure for evaluating the conduction time between electrodes was biased towards longer estimates. What then might explain the fact that in three of five animals, the estimated interval between the onset of the pulse and the

Table 7

Comparison of interelectrode conduction time and onset of effective blocking duration

Subject	Interelectrode Conduction Time (msec)	Effective Blocking Duration (msec)
D-34	1.0	1.4 - 2.0
D-29	0.6	1.0 - 1.4
D-6	1.4	1.4 - 2.0
D-2	2.15	1.0 - 1.4
M-20	0.8	0.25 - 1.0

onset of the block exceeded the estimated interelectrode conduction time? A plausible explanation is based on the concept of utilization time. At long pulse durations, neurons nearest the tip are likely excited earlier during the pulse than neurons farther from the tip. As a result, the arrival of impulses at the hyperpolarized region may be significantly staggered. In addition, the degree of hyperpolarization in elements under the anode will depend on the distance of cells from the tip. Initially, impulses arriving near the tip of the anode have a greater probability of being blocked than impulses arriving in the outer regions of the hyperpolarized field where the current density may be too weak to produce an effective block. Consequently, a longer duration may be required to block impulses conducting far from the tip. The fact that collision effects are usually observed only when the currents at which each electrode is tested are rather high suggests that the fibers common to both fields are located distant from the tip. It is possible, then, that the anodal block in these fibers occurs later than is suggested by the interelectrode conduction time due to the increased utilization time at long pulse durations and the decreased strength of the hyperpolarization block as distance from the anode is increased. Because only short pulse durations (0.1 msec) are used in collision tests, differences in utilization time cannot make a detectable contribution to

the results.

Referring back to Table 7, D-2 is the single subject in which the range of durations corresponding to block onset was less than the estimate of interelectrode conduction time. One possibility is that the conduction time in this subject was seriously overestimated. Recall that the choice of criteria for determining recovery from collision and refractoriness may significantly alter the estimate of interelectrode conduction time because the slopes of the functions from single- and double-electrode tests are not parallel. In D-2, the difference in the slopes is particularly large (see Figures 7 and 8), adding even greater uncertainty to the estimate of conduction time.

An alternative possibility is that the effective blocking field at the VTA was larger than the effective stimulation field generated in collision and refractory period tests at this site. In strength-duration tests, the size of the anodal field depends on the current at the cathode. For subject D-2, the cathode current in the $LH^- SS^+$ and $LH^- VTA^+$ tests was 1400 μA , whereas the current at which the VTA was tested in Experiments 1 and 2 was only 315 μA .

As pointed out earlier, the size of the blocking field may be significantly less than the stimulation field. Nonetheless the more than four-fold difference in the LH^- and VTA^- cathode currents in D-2 may have overcome this bias and caused the size of the blocked region in the VTA to

exceed the size of the cathodal stimulation field that was generated at this site in Experiment 1. If this explanation is correct, then one way to account for the difference in the estimated interelectrode conduction time and the interval between the onset of the pulse and the onset of the block is that stimulation with the $LH^- VTA^+$ configuration blocked faster conducting elements triggered by the LH cathode that were not stimulated by the VTA cathodal field in collision tests. In other words, some of the first stage neurons undergoing hyperpolarization block were different from the neurons that underwent collision block.

One feature of the strength-duration data that is especially apparent when the ratios of the currents correspond to LH^- stimulation are plotted is the rather gradual convergence of the strength-duration functions in Figure 11. This is most evident in the results of subjects D-2 and D-34. This effect may also be explained by the concept of utilization time. If the impulses propagating towards the hyperpolarized region arrived almost simultaneously, then the rise in the ratio values would be abrupt. That is, a step-like profile reminiscent of the collision functions in Figure 7 would be expected. Instead, the LH^- ratio data suggest that the magnitude of the block increases over a wide range of pulse durations in some subjects, perhaps due to the successive arrival at the hyperpolarized regions of impulses triggered after

increasing utilization times.

The position of the strength-duration curves on the ordinate

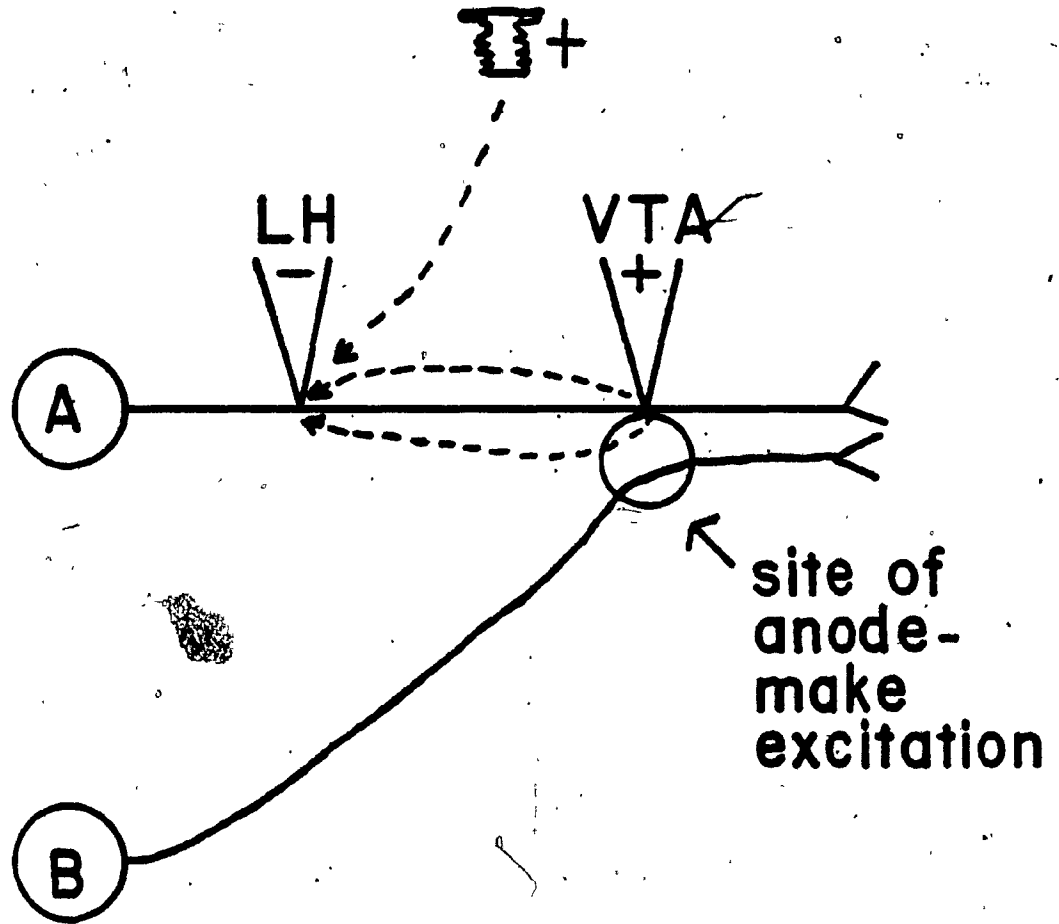
At short pulse durations, the required current was often much lower when two depth electrodes were used than when a depth electrode/skull screw combination was used. This effect manifests itself in the ratio data plotted in Figures 11 and 12 as \log_{10} values at the short pulse durations that are markedly different from zero. The effect is most pronounced in the $LH^- VTA^+$ case. Note that in Figures 11 and 12 (left panel), the required current for short pulse durations in the $LH^- VTA^+$ condition is almost always less than that for the $LH^- SS^+$ condition. There may be at least two reasons for this effect. First, the difference in the LH^- strength-duration functions at pulse durations too short to interfere with conduction may reflect the lower threshold of MFB fibers to longitudinal current flow. Fibers parallel to the alignment of the electrode tips are more easily stimulated than fibers perpendicular to the alignment of the tip due to the increased voltage gradient set up along the fiber (Ranck, 1981; Rushton, 1927). If that is the case, then why wasn't the required current also reduced to the same degree when the $VTA^- LH^+$ condition was tested? In order to answer this, a highly arbitrary geometric arrangement would have to be contrived and the exact path of current flow known. Although this explanation

may be correct, it is not very appealing at this time. An additional study will have to be conducted to assess the effect of the angle of current flow with these electrode configurations.

The second possibility is that the contribution of firings due to anode-make excitation is greater at the VTA than at the LH site. Once again, this mechanism is proposed only to account for the difference in the required currents in the $LH^- SS^+$ and $LH^- VTA^+$ conditions at short pulse durations. Although anodal pulses induce a hyperpolarization at the electrode tip, they may also excite tissue by remote depolarization. That is, the hyperpolarizing currents entering at the tip must exit at another region further from the tip. If the exiting currents are sufficiently dense, then the additional firings they produce will contribute to the total level of excitation and reduce the current required to maintain criterial performance. It is important to note that the subpopulation excited via the anode-make mechanism cannot be the same as the subpopulation that courses past both electrode tips. This is illustrated in Figure 13. While cell A courses by both electrodes, cell B does not and can only contribute firings due to anode-make at the VTA site. When current enters at the VTA or the skull screw, the exiting current is focused at the LH. The LH electrode is too far from the subpopulation activated via the anode-make mechanism, represented by cell B in Figure

Figure 13: Hypothetical example to illustrate anode-make excitation. Cell A is stimulated by both electrodes; cell B is only stimulated by the VTA when it serves as an anode.

ANODE-MAKE EXCITATION



13, to fire the cells when the skull screws serve as the anode. In other words, this mechanism would cause a greater number of first stage neurons to fire when a current was passed from the depth anode to the depth cathode than when a current of the same magnitude was passed from the skull screws to the depth electrode.

If this explanation is correct and one takes into account the currents used in this study, it is not surprising that the VTA electrode should contribute more anode-make excitation than the LH. Recall that in the strength-duration tests, the size of the current leaving the depth anode depends on the current used in the collision experiment when the other depth electrode served as the cathode, and therefore may not correspond to the same stimulation fields generated in collision and refractory period tests. In the collision experiment, the LH currents were generally much greater than the VTA currents. The currents leaving the VTA electrode in the LH⁻ VTA⁺ condition were much larger than the currents leaving the LH in the LH⁺ VTA⁻ condition. Hence anode-make excitation was more likely to contribute to the results from the former case than from the latter.

Aspects of the data in Figures 11 and 12 do appear to support the "anode-make" hypothesis. Subjects with the largest discrepancies between the LH and VTA currents in the collision experiment (e.g., D-2) tend to show the biggest

difference in required currents, especially when the LH electrode served as the cathode and either the VTA electrode or the skull screws served as the anode. Moreover, the direction of the effect is consistent. That is, the difference between the required currents was largest in the LH⁻ comparisons where the highest currents were employed.

Two puzzling features of the data, however, cannot be explained by anode-make excitation. In the one subject with equal LH and VTA currents in the collision experiment (D-29), there is a noticeable difference in the currents required in the LH⁻ VTA⁺ and LH⁻ SS⁺ conditions but little difference in the VTA⁻ LH⁺ and VTA⁻ SS⁺ conditions. In contrast, the anode-make explanation predicts that the magnitude of the difference be similar in the LH⁻ and VTA⁻ conditions.

The second problem concerns the cases where the curves from the LH⁻ SS⁺ and VTA⁻ SS⁺ configurations lie below the curves obtained with the depth electrodes. This can be clearly seen in Figure 11k and in Figure 12, a and b. Again, according to the anode-make hypothesis, the required current in tests where the skull screw served as the anode should never be less than the required current in tests where the depth electrode served as the anode since no anode-make contribution is expected from the skull screw anode.

One issue raised by the discrepancy between the LH

and VTA currents pertains to the possible bias against detecting an ascending projection. It is possible that in the $VTA^- LH^+$ condition, the blocking field at the LH may have been too small to recruit the fibers that normally participate in collision effects. The results of the one subject with equal currents (D-29) weakens this view. In this subject, the LH and VTA currents were equal in value for strength-duration data collected at high and low current ranges. As can be seen from Figure 11f, the ratio of the LH required currents approaches zero only at the long pulse durations in contrast to the VTA ratio which remains flat at all durations. Thus, even in the case where the collision and strength-duration currents were the same and matched between electrodes, no ascending component of the directly stimulated reward-relevant pathway was found.

Numerical description of the shape differences

The inference that the neurons responsible for the collision effect project rostrocaudally is based on the shapes of the strength-duration functions obtained in Figures 11 and 12. It is apparent from a visual inspection of the data that the high current curves in the LH^- conditions in Figure 11 are not parallel while all other pairs of curves are very nearly parallel. However, in order to numerically assess the difference in the shapes of the strength-duration functions, chronaxie estimates were

obtained by fitting hyperbola to each of the functions in Figures 11 and 12. The hyperbola has been found to provide an acceptable fit to MFB strength-duration data (Gallistel, 1978; Matthews, 1977) and is convenient to linearize. Recall that the chronaxie describes the shape of the hyperbolic function. Functions with more gradual slopes on the logarithmic coordinate system used in the left-hand panels of Figures 11 and 12 should have the lower chronaxie values.

The hyperbolic equation has the form:

$$I = r (1 + c/d),$$

where I = intensity,

r = rheobase,

c = chronaxie,

and d = duration.

Multiplying through by duration yields:

$$Id = rd + rc,$$

where Id = charge,

r = slope of the function,

and rc = intercept of the function.

To obtain the chronaxie, the intercept is divided by the slope.

The chronaxie estimate for each strength-duration

curve in Figures 11 and 12 is listed in Table 8. The estimates were derived from a weighted regression analysis (BMDPLR). The average chronaxie estimate for each stimulation condition and current level has also been included in the table. Because of the few extreme scores, the median estimate was noted as well.

Note that in every subject, the chronaxie of the $LH^- VTA^+$ curve from the high current condition was substantially less than the chronaxie for the corresponding $LH^- SS^+$ condition. The median chronaxie value for the $LH^- VTA^+$ condition, 0.61 msec, is less than half the median chronaxie for the $LH^- SS^+$ condition, 1.62 msec. This difference was statistically significant ($p < .05$; Sign test). No significant difference was found when the VTA electrode was used as the cathode and either the skull screws or the second electrode was the anode. The median chronaxie values for the remaining comparisons (low current data) differ by no more than 11%.

In this analysis, the shape of each strength-duration curve was described by a single number, the chronaxie. The legitimacy of reducing each curve to a single number depends on how well the hyperbola fits the strength-duration function. The Pearson r values obtained from the analysis (Table 9) were higher than 0.90 in 32/36 curves and higher than 0.80 in 35/36 curves.

It is somewhat troubling that the chronaxie

Table 8

Chronaxies obtained from weighted linear regression test on charge vs pulse duration

Subject	High Current Data			
	LH ⁻ SS ⁺	LH ⁻ VTA ⁺	VTA ⁻ SS ⁺	VTA ⁻ LH ⁺
D-34	6838	754	1897	2025
D-29	1284	595	699	712
D-6	1622	573	704	715
D-2	2271	721	1379	1162
M-20	837	610	662	788
Average	2571	651	1068	1081
Median	1622	610	704	788
Subject	Low Current Data			
	LH ⁻ SS ⁺	LH ⁻ VTA ⁺	VTA ⁻ SS ⁺	VTA ⁻ LH ⁺
D-34	893	687	1260	1067
D-29	1295	1173	825	947
D-6	1168	1643	1031	914
SL-19	1540	1264	780	1229
Average	1224	1192	974	1039
Median	1232	1219	928	1007

Table 9

Pearson r values obtained from weighted linear regression test on charge vs pulse duration

High Current Data				
Subject	LH ⁻ SS ⁺	LH ⁻ VTA ⁺	VTA ⁻ SS ⁺	VTA ⁻ LH ⁺
D-34	0.52	0.99	0.85	0.82
D-29	0.93	0.98	0.97	0.96
D-6	0.96	0.98	0.98	0.98
D-2	0.86	0.99	0.99	0.97
M-20	0.99	0.98	0.99	0.99

Low Current Data				
Subject	LH ⁻ SS ⁺	LH ⁻ VTA ⁺	VTA ⁻ SS ⁺	VTA ⁻ LH ⁺
D-34	0.91	0.95	0.95	0.96
D-29	0.98	0.98	0.98	1.00
D-6	0.94	0.99	0.97	0.98
SL-19	0.92	0.90	0.95	0.95

differences obtained between the high current $LH^- SS^+$ and $LH^- VTA^+$ conditions were the highest in the case (D-34) where the strength-duration curve was most poorly fit by a hyperbola. Nonetheless, the group difference cannot be attributed to the poor fit since large differences were found in subjects where the fits were excellent (D-6 and D-29).

These results confirm the visual analysis of the shapes of the strength-duration curves in Figures 11 and 12.

Anode-make excitation revisited

An examination of the data in Table 8 reveals that the chronaxies obtained from the strength-duration curves representing the $VTA^- SS^+$ condition are shorter than the chronaxies obtained from the strength-duration curves representing the $LH^- SS^+$ condition. Hence, it might be argued that the short chronaxies obtained from the results of the electrode configuration interpreted to produce a block are instead due to the combination of long chronaxie elements recruited at the LH cathode and short chronaxie elements fired by the VTA anode. Since in the model, the $LH^- VTA^+$ electrode configuration stimulates neurons at two sites, one near the LH electrode and one near the VTA electrode, the resulting chronaxie should lie between the chronaxie values obtained from the strength-duration functions corresponding to the LH and VTA

cathode/skull-screw combination. This is not the case. As can be seen from Table 8, for every subject, the chronaxie value listed under the $LH^- VTA^+$ column was always less than the chronaxie listed under the $VTA^- SS^+$ column.

Finally, if one were to entertain the anode-make hypothesis as the sole reason for the differences in the shapes of the curves representing the $LH^- SS^+$ and $LH^- VTA^+$ stimulation conditions, one would have to explain two very puzzling results. The first concerns the finding that the LH and VTA electrodes stimulate some of the same neurons. Assuming that this interpretation is correct, why would the anodal-induced hyperpolarization fail to block impulses triggered in the same fibers and why would the difference in the shapes of the curves disappear when currents corresponding to an absence of collision-like effects are tested in the direction experiment? This would seem even more surprising if one takes into account the currents used in the direction test. Especially in the case of D-2, the current leaving the cathode and entering the anode was more than four times the current used at the VTA in collision-tests. Given the high current levels, it would be difficult to reconcile the absence of a block in my data.

It is possible that neurons with shorter chronaxies, activated in the region of the VTA by the mechanism of anodal-make excitation, contribute to the shape of the strength-duration function obtained from $LH^- VTA^+$

stimulation. Nonetheless, it is extremely unlikely that this is the only reason for the difference in the shape. Accordingly, there appears to be no reasonable way to account for the differences in the shape without appealing to the anodal-block effect.

Significance of these findings

The results of the experiments presented in this thesis suggest that the neurons responsible for the collision effects conduct signals in the rostrocaudal direction. Only one electrode configuration was consistent with this interpretation - when the LH served as the cathode and the VTA served as the anode. Nonetheless, the contribution of ascending fibers to the pathway comprising the directly stimulated reward-relevant bundle cannot be ruled out. In several of my subjects, the difference in the currents between the LH and VTA was biased towards the detection of a descending pathway. However, in the one subject with equal currents (D-29), no ascending component was observed. Thus, the best explanation for the data in Experiment 3 is that the first stage reward fibers are characterized by a descending bundle.

The implications of this finding are several. First, it reinforces the idea that the neurons responsible for the rewarding effect that contribute to collision effects are non-dopaminergic. Second, combined with the

2-deoxy-d-glucose procedure for detecting metabolic activity, it provides a powerful guide towards the electrophysiological identification of first-stage reward elements. The descending components of the MFB that look most promising originate in the lateral preoptic area, septum, and form the MFB path neurons (Nieuwenhuys et al., 1982). Finally, together with estimates of conduction velocity, refractory period, and strength-duration properties, the finding presented here provides a good starting point for assessing the neural organization of brain-stimulation reward.

REFERENCES

- Accornero, N., Bini, G., Lenzi, G. L., & Manfredi, M. (1977). Selective activation of peripheral nerve fibre groups of different diameter by triangular shaped stimulus pulses. Journal of Physiology, 273, 539-560.
- Adrian, E. D., & Lucas, K. (1912). On the summation of a propagated disturbance in nerve and muscle. Journal of Physiology, 44, 68-124.
- Bielajew, C., & Fouriez, G. (1983). Mediodorsal thalamic self-stimulation: Excitability characteristics. Manuscript in preparation.
- Bielajew, C., Jordan, C., Ferme-Enright, J., & Shizgal, P. (1981). Refractory periods and anatomical linkage of the substrates for lateral hypothalamic and periaqueductal gray self-stimulation. Physiology and Behavior, 27, 95-104.
- Bielajew, C., Lapointe, M., Kiss, I., & Shizgal, P. (1982). Absolute and relative refractory periods of the substrates for lateral hypothalamic and ventral midbrain self-stimulation. Physiology and Behavior, 28, 125-132.
- Bielajew, C., & Shizgal, P. (1980). Dissociation of the substrates for medial forebrain bundle self-stimulation and stimulation-escape using a two-electrode stimulation technique. Physiology and Behavior, 25, 707-711.
- Bielajew, C., & Shizgal, P. (1982). Behaviorally derived

measures of conduction velocity for rewarding medial forebrain bundle stimulation. Brain Research, 237, 107-119.

Bielajew, C., Walker, S., & Fouriez, G. (1983).

Refractoriness of reward-relevant neurons in the nucleus accumbens and adjacent structures. Society for Neuroscience Abstracts, 9, in press.

Bishop, M. P., Elder, S. T., & Heath, R. G. (1963).

Intracranial self-stimulation in man. Science, 140, 394-396.

Bower, G. H., & Miller, N. E. (1958). Rewarding and

punishing effects from stimulating the same place in the rat's brain. Journal of Comparative and Physiological Psychology, 51, 669-674.

Boycott, A. E. (1899). Note on the muscular response to two

stimuli of the sciatic nerve (frog). Journal of Physiology, 24, 144-145.

Boyd, E. S., & Gardner, L. C. (1962). Positive and negative

reinforcement from intracranial stimulation of a teleost. Science, 136, 648-649.

Bramwell, J. C., & Lucas, K. (1911). On the relation of the

refractory period to the propagated disturbance in nerve. Journal of Physiology, 42, 495-518.

Caggiula, A. R., & Hoebel, B. G. (1966). "Copulation-reward

site" in the posterior hypothalamus. Science, 153, 1284-1285.

- Cooper, R., & Taylor, L. (1967). Thalamic reticular system and central grey: Self-stimulation. Science, 156, 102-103.
- Corbett, D., & Wise, R. (1980). Intracranial self-stimulation in relation to the ascending dopaminergic systems of the midbrain: a moveable electrode mapping study. Brain Research, 185, 1-15.
- Dalsass, M., German, D., & Kiser, R. (1978). Anatomical and electrophysiological examination of neurons in the nucleus A-10 region of the rat. Society for Neuroscience Abstracts, 4, 422.
- Deutsch, J. A. (1964). Behavioral measurement of the neural refractory period and its application to intracranial self-stimulation. Journal of Comparative and Physiological Psychology, 58, 1-9.
- Durivage, A., & Miliaressis, E. (1983). Dissociation of MFB substrates for self-stimulation and exploration. Society for Neuroscience Abstracts, in press.
- Edmonds, D. E., & Gallistel, C. R. (1977). Reward versus performance in self-stimulation: electrode-specific effects of alpha-methyl-p-tyrosine on reward in the rat. Journal of Comparative and Physiological Psychology, 91, 962-974.
- Erlanger, J., & Gasser, H. S. (1937). Electrical signs of neural activity. London: Oxford University Press.
- Eyzaguirre, C., & Fidone, S. (1975). Physiology of the

- nervous system (2nd ed.). Chicago: Year Book Medical.
- Feltz, P., & Albe-Fessard, D. (1972). A study of an ascending nigro-caudate pathway. Electroencephalography and Clinical Neurophysiology, 33, 179-193.
- Fouriezos, G., Hansson, P., & Wise, R. (1978). Neuroleptic induced attenuation of brain stimulation reward in rats. Journal of Comparative and Physiological Psychology, 92, 661-671.
- Fouriezos, G., & Wise, R. (1983). Current-distant relation for rewarding brain stimulation. Submitted to Nature.
- Gallistel, C. R. (1973). Self-stimulation: The neurophysiology of reward and motivation. In J. A. Deutsch (Ed.): The physiological basis of memory. New York: Academic Press.
- Gallistel, C. R. (1978). Self-stimulation in the rat: Quantitative characteristics of the reward pathway. Journal of Comparative and Physiological Psychology, 92, 977-998.
- Gallistel, C. R., Shizgal, P., & Yeomans, J. S. (1981). A portrait of the substrate for self-stimulation. Psychological Review, 88, 228-273.
- Gasser, H. S., & Grundfest, H. (1936). Action and excitability in mammalian A fibers. American Journal of Physiology, 117, 113-133.
- German, D., Dalsass, M., & Kiser, R. (1980). Electrophysiological examination of the ventral tegmental

- (A10) area in the rat. Brain Research, 181, 191-197.
- German, D., & Holloway, F. (1972). Behaviorally determined neurophysiological properties of MFB self-stimulation fibers. Physiology and Behavior, 9, 823-829.
- Gotch, F., & Burch, G. J. (1899). The electrical response of nerve to two stimuli. Journal of Physiology, 2, 410-426.
- Guyenet, P., & Aghajanian, S. (1978). Antidromic identification of dopaminergic and other output neurons of the rat substantia nigra. Brain Research, 150, 69-84.
- Hawkins, R. D., & Chang, J. (1974). Behavioral measurement of the neural refractory periods for stimulus-bound eating and self-stimulation in the rat. Journal of Comparative and Physiological Psychology, 86, 942-948.
- Hawkins, R. D., Roll, P. L., Puerto, A., & Yeomans, J. S. (1983). The post-stimulation excitability cycle in self-stimulation: A functional measurement analysis. Manuscript in preparation.
- Hoebel, B. G. (1974). Brain reward and aversion systems in the control of feeding and sexual behavior. In J. K. Cole and T. B. Sonderegger (Eds.): Nebraska Symposium on Motivation (Vol. 22). Lincoln: University of Nebraska Press.
- Hoebel, B. G., & Teitelbaum, P. (1962). Hypothalamic control of feeding and self-stimulation. Science, 135, 375-377.
- Hoebel, B. G., & Thompson, R. D. (1969). Aversion to lateral hypothalamic stimulation caused by intragastric feeding

- or obesity. Journal of Comparative and Physiological Psychology, 68, 536-543.
- Hu, J. W. (1973). Refractory period of hypothalamic thirst pathway in the rat. Journal of Comparative and Physiological Psychology, 85, 463-468.
- Huston, J., & Borbély, A. (1973). Operant conditioning in forebrain ablated rats by use of rewarding hypothalamic stimulation. Brain Research, 50, 467-472.
- Huston, J., & Borbély, A. (1974). The thalamic rat: General behavior operant learning with rewarding hypothalamic stimulation and effects of amphetamine. Physiology and Behavior, 12, 433-448.
- Kiss, I. (1982). The electrophysiological characteristics of the substrate for brain-stimulation reward in the MFB.
Unpublished Master's thesis.
- Kocsis, J. D., Swadlow, H. A., Waxman, S. G., & Brill, M. H. (1979). Variation in conduction velocity during the relative refractory and supernormal periods: A mechanism for impulse entrainment in central axons. Experimental Neurology, 65, 230-236.
- Kuffler, S., & Vaughan-Williams, E. (1953). Small-nerve junctional potentials. The distribution of small motor nerves to frog skeletal muscle and the membrane characteristics of the fibres they innervate. Journal of Physiology, 121, 289.
- Lucas, K. (1910). Quantitative reseraches on the summation

of inadequate stimuli in muscle and nerve, with observations on the time-factor in electric excitation. Journal of Physiology, 39, 461-475.

Lucas, K. (1913). The effect of alcohol on the excitation, conduction, and recovery process in nerve. Journal of Physiology, 46, 470-505.

Lucas, K. (1917). On summation of propagated disturbances in the claw of astacus, and on the double neuro-muscular system of the adductor. Journal of Physiology, 51, 1-35.

MacMillan, C., & Shizgal, P. (1983). Self-stimulation of the lateral hypothalamus and substantia nigra: Excitability characteristics of the directly stimulated substrates. Canadian Psychological Association meetings, Winnipeg, June 1983.

Maeda, H., & Mogenson, G. (1980). An electrophysiological study of inputs to neurons of the ventral tegmental area from the nucleus accumbens and medial preoptic-anterior hypothalamic areas. Brain Research, 197, 365-377.

Matthews, G. (1977). Neural substrate for brain stimulation reward in the rat: Cathodal and anodal strength-duration properties. Journal of Comparative and Physiological Psychology, 91, 858-874.

Matthews, G. (1978). Strength-duration properties of single units driven by electrical stimulation of the lateral hypothalamus in rats. Brain Research Bulletin, 3, 171-174.

- Mendelson, J. (1967). Lateral hypothalamic stimulation in satiated rats: The rewarding effects of self-induced drinking. Science, 157, 1077-1079.
- Miliaressis, E., & Rompré, P. P. (1980). Self-stimulation and circling: Differentiation of the neural substrata by behavioral measurement with the use of a double pulse technique. Physiology and Behavior, 25, 939-943.
- Milner, P. N. (1978). Tests of two hypotheses about summation of rewarding brain stimulation. Canadian Journal of Psychology, 32, 95-105.
- Monnier, M. (1970). Functions of the nervous system, (Vol. 2). Amsterdam: Elsevier, pp. 49-60.
- Mundl, W. J. (1980). A constant-current stimulator. Physiology and Behavior, 24, 991-993.
- Nakajima, S. (1972). Effects of intracranial chemical injections upon self-stimulation in the rat. Physiology & Behavior, 8, 741-746.
- Nauta, W. J. H., & Domesick, V. B. (1978). Cross roads of limbic and striatal circuitry: Hypothalamo-nigral connections. In K. E. Livingstone and O. Hornykiewicz (Eds.): Limbic mechanisms. New York: Plenum.
- Neter, J., & Wasserman, W. (1974). Applied linear statistical models. Homewood, Illinois: Richard D. Irwin.
- Nieuwenhuys, R., Geeraedts, L., & Veening, J. (1982). The medial forebrain bundle of the rat. I. General introduction. Journal of Comparative Neurology, 206,

49-81.

Noble, D., & Stein, R. (1966). The threshold conditions for initiation of action potentials by excitable cells.

Journal of Physiology, 187, 129-162.

Olds, M., & Olds, J. (1969). Effects of lesions in medial forebrain bundle on self-stimulation behavior. American Journal of Physiology, 217, 1253-1264.

Pellegrino, L. J., Pellegrino, A. S., & Cushman, A. J. (1979). A stereotaxic atlas of the rat brain (2nd ed.). New York: Plenum Press.

Ranck, J. B., Jr. (1975). Which elements are excited in electrical stimulation of mammalian central nervous system: a review. Brain Research, 98, 417-440.

Ranck, J. B., Jr. (1981). Extracellular stimulation. In M. M. Patterson and R. P. Kesner (Eds.): Electrical stimulation research techniques. New York: Academic Press.

Rolls, E. T. (1973). Refractory period of neurons directly excited in stimulus-bound eating and drinking in the rat. Journal of Comparative and Physiological Psychology, 82, 15-22.

Rolls, E. T., Burton, M. J., & Mora, F. (1980). Neurophysiological analysis of brain-stimulation reward in the monkey. Brain Research, 194, 339-357.

Rolls, E. T., & Kelley, P. (1972). Neural basis of stimulus-bound locomotor activity in the rat. Journal of

Comparative and Physiological Psychology, 81, 173-182.

Rompré, P. P., & Miliaressis, E. T. (1980). A comparison of the excitability cycles of the hypothalamic fibers involved in self-stimulation and exploration. Physiology and Behavior, 24, 995-998.

Rushton, W. A. H. (1927). Effect upon the threshold for nervous excitation of the length of nerve exposed and the angle between current and nerve. Journal of Physiology, 63, 357-377.

Rushton, W. (1930). Excitable substances in the nerve-muscle complex. Journal of Physiology, 70, 317-337.

Schenk, S., & Shizgal, P. (1982). The substrates for lateral hypothalamic and medial prefrontal cortex self-stimulation have different refractory periods and show poor spatial summation. Physiology and Behavior, 28, 133-138.

Schenk, S., & Shizgal, P. (1983). Self-stimulation of the prefrontal cortex: Strength-duration characteristics. Submitted to Physiology and Behavior.

Schmitt, R., Sandner, G., & Karli, P. (1976).

Caractéristiques fonctionnelles des systèmes de renforcement: étude comportementale. Physiology and Behavior, 16, 419-429.

Shizgal, P., Bielajew, C., Corbett, D., Skelton, R., & Yeomans, J. S. (1980). Behavioral methods for inferring anatomical linkage between rewarding brain stimulation

- sites. Journal of Comparative and Physiological Psychology, 94, 227-237.
- Shizgal, P., Howlett, S., & Corbett, D. (1979). Behavioral inference of current-distance relationships in rewarding electrical stimulation of the rat hypothalamus. Canadian Psychological Association meetings, Québec City, June, 1979.
- Shizgal, P., Bielajew, C., & Kiss, I. (1980). Anodal hyperpolarization block technique provides evidence for rostro-caudal conduction of reward related signals in the medial forebrain bundle. Society for Neuroscience Abstracts, 6, 422.
- Shizgal, P., Kiss, I., & Bielajew, C. (1982). Electrophysiological and psychophysiological studies of the substrate for brain stimulation reward. In B. Hoebel and D. Novin (Eds.): The neural basis of feeding and reward. Brunswick, Maine: Haer Institute.
- Shizgal, P., & Matthews, G. (1977). Electrical stimulation of the rat diencephalon: Differential effects of interrupted stimulation on on- and off-responding. Brain Research, 129, 319-333.
- Silva, L., Vogel, J., & Corbett, D. (1982). Frontal cortex self-stimulation: Evidence for independent substrates within areas 32 and 24. Society for Neuroscience Abstracts, 8, 625.
- Skelton, R. W., & Shizgal, P. (1980). Parametric analysis of

ON- and OFF- responding for hypothalamic stimulation.

Physiology and Behavior, 25, 699-706.

Stein, L. (1969). Chemistry of purposive behavior. In J.

Tapp (Ed.): Reinforcement and behavior. New York:

Academic Press.

Stellar, J., Brooks, F., & Mills, L. (1979). Approach and

withdrawal analysis of the effects of hypothalamic

stimulation and lesions in rats. Journal of Comparative

and Physiological Psychology, 93, 446-466.

Stellar, J. R., Illes, J., & Mills, L. E. (1982). Role of

ipsilateral forebrain in lateral hypothalamic stimulation

reward in rats. Physiology and Behavior, 1982, 1089-1097.

Stellar, J., & Neeley, S. (1982). Reward summation function

measurements of lateral hypothalamic stimulation reward:

Effects of anterior and posterior medial forebrain bundle

lesions. In B. Hoebel and D. Novin (Eds.): The neural

basis of feeding and reward. Brunswick, Maine: Haer

Institute.

Swadlow, H. A., & Waxman, S. E. (1978). Activity-dependent

variations in the conduction properties of central axons.

In S. E. Waxman (Ed.): Physiology and pathobiology of

central axons. New York: Raven Press.

Swett, J., & Bourassa, C. (1981). Electrical stimulation of

peripheral nerve. In M. Patterson and R. Kesner (Eds.):

Electrical stimulation research techniques. New York:

Academic Press.

- Szabo, I., Lénard, L., & Kosarás, B. (1974). Drive decay theory of self-stimulation: Refractory periods and axon diameters in hypothalamic reward loci. Physiology and Behavior, 12, 329-343.
- Szabo, I., Nad, E., & Szabo, C. (1972). Pole reversals and hypothalamic self-stimulation: Ascending spread of rewarding excitation. Physiology and Behavior, 9, 147-150.
- Takigawa, M., & Mogenson, G. (1977). A study of inputs to antidromically identified neurons of the locus coeruleus. Brain Research, 135, 217-230.
- Veening, J., Swanson, L., Cowan, M., Nieuwenhuys, R., & Geeraedts, L. (1982). The medial forebrain bundle of the rat. II. An autoradiographic study of the topography of the major descending and ascending components. Journal of Comparative Neurology, 206, 82-108.
- Waxman, S., & Bennett, M. (1972). Relative conduction velocities of small myelinated fibers in the central nervous system. Nature, 238, 217-219.
- Yeomans, J. S. (1974). Behavioral measurement of neural temporal excitability changes including refractory periods: A re-evaluation. Unpublished Doctoral thesis.
- Yeomans, J. S. (1975). Quantitative measurement of neural post-stimulation excitability with behavioral methods. Physiology and Behavior, 15, 593-602.
- Yeomans, J. S. (1979). The absolute refractory periods of

self-stimulation neurons. Physiology and Behavior, 22, 911-919.

Yeomans, J., & Koopmans, H. (1974). On the directionality of medial forebrain bundle fibers mediating self-stimulation. Science, 183, 102.

Yeomans, J. S., Matthews, G., Hawkins, L. D., Bellman, K., & Doppelt, H. (1979). Characterization of self-stimulation neurons by their local potential summation properties. Physiology and Behavior, 22, 921-929.

Yeomans, J., & Mercouris, N. (1983). Refractory period estimates vary as a function of current and electrode tip surface area. Canadian Psychological Association meetings, Winnipeg, June 1983.

Yim, C., & Mogenson, G. (1980). Electrophysiological studies of neurons in the ventral tegmental area of Tsai. Brain Research, 181, 301-313.

